Escuela
Politécnica
Superior

Neural part-of-speech tagging

Bachelor's Degree in Computer Engineering

Bachelor's Thesis

Author:
Francisco de Borja Valero

Supervisors:
Juan Antonio Pérez Ortiz
Felipe Sánchez Martínez

Universitat d'Alacant
Universidad de Alicante

November 2018

Resumen

En este proyecto proponemos la implementación de un sistema desambiguador de categorias léxicas utilizando redes neuronales recurrentes. Para ello, inicialmente estudiamos los fundamentos teóricos de este tipo de redes neuronales. Posteriormente, proponemos tres arquitecturas diferentes para solventar la desambiguación de palabras ambiguas. Finalmente, obtenemos un sistema capaz de desambiguar con un 93.5 % de acierto total y con un 83.2 % de acierto en palabras ambiguas en la sección del Wall Street Journal perteneciente al corpus del Penn Treebank.

Abstract

In this work, we propose the implementation of a part-of-speech tagging system using recurrent neural networks. For that purpose, initially we study the theoretical fundamentals of that kind of neural networks. Next, we propose three different architectures in order to disambiguate ambiguous words. Finally, we achieve a system able to disambiguate with a 93.5% total accuracy and with 83.2% accuracy on ambiguous words with the section of Wall Street Journal that belongs to the Penn Treebank corpus.

Contents

List of Figures

List of Tables

Acronyms

BPTT backpropagation through time.

CUDA Compute Unified Device Architecture.

cuDNN CUDA Deep Neural Network Library.

DL deep learning.

GCP Google Cloud Platform.

GPU graphics processing unit.

GRU gated recurrent unit.

HMM hidden Markov model.

IE information extraction.

LSTM long short term memory.

MEMM maximum entropy Markov model.

ML machine learning.

MLP multilayer perceptron.

NER name entity recognition.

NLP natural language processing.

NLTK natural language toolkit.

NN neural network.

PoS part-of-speech.

ReLU rectifier linear unit.

RNN recurrent neural network.

Seq2Seq sequence to sequence.

SGD stochastic gradient descent.

WSJ Wall Street Journal.

Chapter 1

Introduction

This first chapter introduces the main topic of this work. First, we present an overview of the problem and comment on the approaches used in the past to tackle *part-of-speech* tagging (see section 1.1). Next, we describe ambiguity classes as a method to represent the words (see section 1.2). Finally, we give the structure of the project (see section 1.3).

1.1. Overview

Part-of-speech (PoS) tagging is the task of assigning a PoS tag (a lexical category) to each word in a sentence. This task belongs to the *natural language processing* (NLP) field, and provides very useful information to other NLP tasks, such as *information extraction* (IE) or *name entity recognition* (NER), among others [13].

In a natural language like English, a particular word can be assigned different PoS tags, depending on its context. Ambiguous words are frequently found in a sentence; about 1/3 of the words in running texts are ambiguous. The next two sentences: "My sister **can** speak three languages" and "I have a **can** of beer", contain the same word "can", but having different lexical categories. In the first one, "can" is a verb and in the second one is a noun; therefore in English the word "can" is ambiguous. The aim of a PoS tagger is, given a source sentence, disambiguate those words which are ambiguous by taking into account the context in which they appear.

First PoS tagging systems were rule-based [4]. Over the years, the rules of those systems became more complex [5], and on top of that, appeared stochastic models like

hidden Markov models (HMM) [6] and *maximum entropy Markov models* (MEMM) [23], which outperform the results of rule-based systems. At the end of the nineties, *neural networks* (NN) were emerging, and were used by some researchers [25], [22] obtaining interesting results; however the high computational cost of training them made the research community to focus mainly on stochastic models rather than NN models.

Nowadays, the use of this NN models are arising again; unlike before, today we dispose of high performance computers. In recent years, many researches in NN models has appeared. In this work we propose to retake those old architectures [22] and update them to current models and programming frameworks. Moreover, new architectures are proposed.

1.2. Ambiguity classes

Usually, the input to PoS tagging is not an identifier or a representation of a word; typically it is a word class. In this specific problem, the word class is an *ambiguity class* that is the set of all PoS tags that a given word can be assigned. In order to get the ambiguity classes, first we have to process the relation between the words and their PoS tags in a training corpus. In this corpus, each word has assign its respective PoS tag (disambiguate corpus). In the training corpus, the same word can be found with different PoS tags. Therefore, the words that share the same set of PoS tags belong to the same ambiguity class as "the":{DT} and "an":{DT}. Also, when this ambiguity class has more than one PoS tag as "telecommunications":{NN, NNS}; it is said to be ambiguous.

The approaches used above are useful when a given word has been seen in a training corpus. But there is a problem when a word is unknown: it has not been seen in the training corpus. The basic approach is to create an ambiguity class for the unknown words containing all PoS tags available in the tagset. In this way, the tagger decides which is the most promising PoS tag. An alternative to this approach consist of including in the ambiguity class for unknown words only those PoS tags that belong to open categories: nouns, verbs, adjectives and adverbs; because normally, when a new word is added to the vocabulary of a language it belongs to one of these open categories.

Another approach used to reduce the number of possible tags for unknown words consist of using a morphological guesser [19] before running any tagging method. Also there are more complex methods taking into account the probabilities of the suffixes and ending of words an other features to restrict the set of PoS tags. Another approach is to count the occurences of words along the training set, splitting them in regular (frequent) and rare word (less than five occurences); in this way unknown words are treated as if they were rare words [27].

1.3. Outline

This dissertation is structured as follows. Chapter 2 provides the theoretical background required to understand *recurrent neural networks* (RNN). Chapter 3 shows the framework and resources used in this project. Chapter 4 explains the way of encoding ambiguity classes and the proposed architectures. Chapter 5 describes the naive baselines, shows results and other aspects related with experimentation. Finally, chapter 6 presents the conclusions of the project and future work.

Chapter 2

Background

In this second chapter, the online course "Deep Learning Specialization" by Andre Ng[1] has been fundamental in order to clearly explain the basics of *deep learning* (DL): DL is a subset of *machine learning* (ML) whose models have several layers of neurons capable of learning tasks from data.

2.1. Neural Networks

Recurrent neural networks (RNN) are a neural model very popular for dealing with tasks involving sequence processing. Before explaining them, it is necessary to introduce first the *feedforward* model. These models tries to imitate the behaviour of neurons in the human brain.

Figure 2.1 shows a *multilayer perceptron* (MLP) [15] which is constituted by an input layer with two neurons that represent the features of the input data. It is followed by two hidden layers with three and four neurons respectively, and an output layer with only one neuron whose activation value is the prediction $\hat{y}$. A neural layer is represented by a matrix, whose elements are parameters, also know as weights. The shape of the weight matrix in layer l is $W^l \in \mathbb{R}^{H^l \times H^{l-1}}$, where H^l and H^{l-1} are the number of neurons in the current and previous layer respectively. In all layers additional weights exist whose input is always 1. These weights are known as bias $\mathbf{b}^l \in \mathbb{R}^{H^l}$ and its size corresponds to the number of neurons in the corresponding layer. Its contribution is crucial for the training (see section 2.2), because it allows to shift the activation output

[1] https://www.coursera.org/specializations/deep-learning

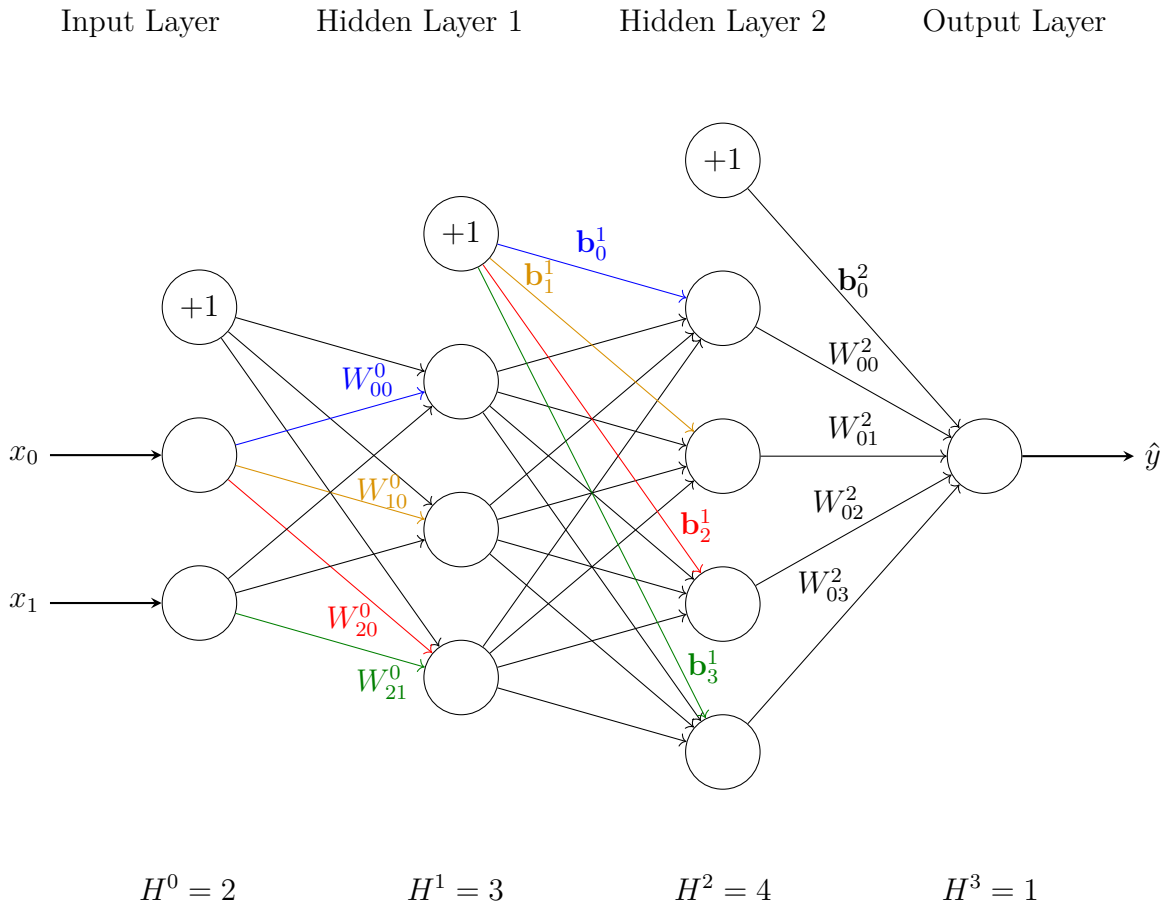

Figure 2.1: Example of a MLP.

in one direction or another for obtaining a successful training.

Equation below shows the operation performed by layer l, where W^l and $\mathbf{b}^l$ are the weights of the current layer and $\mathbf{z}^{l-1}$ is the activation output of the previous layer. Linear combination of previous parameters are introduced in a nonlinear activation function f. In section 2.1.1 some activations functions used by *neural network* layers will be explained with more detail.

$$\mathbf{z}^l = f(W^l \mathbf{z}^{l-1} + \mathbf{b}^l) \tag{2.1}$$

In order to maximize the high performance of existing computers, it is very common to use vectorization principles, thus replacing loops with matrix operations; where m samples are processed simultaneously instead one. Therefore, the shape of input data will be $X \in \mathbb{R}^{H^0 \times m}$, where H^0 is the number of features of the input data, and the shape of the expected output will be $\hat{y} \in \mathbb{R}^{H^L \times m}$, where H^L is the number of neurons in the output layer.

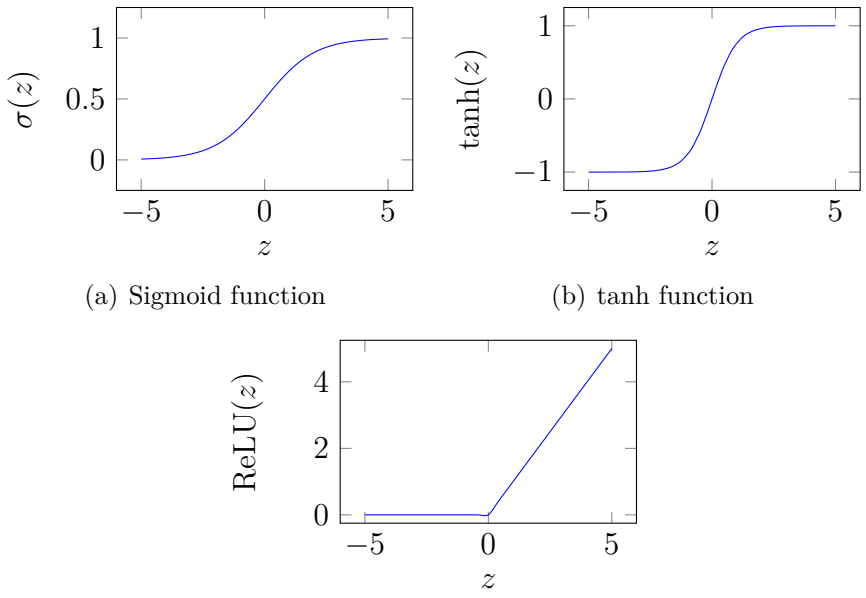

(a) Sigmoid function

(b) tanh function

(c) Rectifier function

Figure 2.2: Activation functions.

2.1.1. Activation functions

Feedforward computation (see section 2.1) allows us to solve non-trivial pattern matching problems thanks to the use of nonlinear functions. In this section the most popular activation functions are described. They are applied to the output of the *neural network* layers; depending on the output, it will be more recommendable to use one or another.

The output value of the *sigmoid* is in $[0, 1]$; normally it is used in the output layer in problems like binary classification or regression where predictions must be in that domain. *Rectifier linear unit* (ReLU) is commonly used in hidden layer because of its special nonlinearity, as its output is always equal or higher than zero, therefore computationally it is simple. The last popular activation function is *hyperbolic tangent* (tanh), whose output is in $[-1, 1]$. Normally, it is used in hidden layers or when a prediction is necessary in that domain. Figure 2.2 shows the behaviour of the three nonlinear functions commented and their analytical forms are shown in the next equations:

$$\sigma(x) = \frac{1}{1 + \exp(-z)} \tag{2.2}$$

$$\tanh(x) = \frac{\exp(z) - \exp(-z)}{\exp(z) + \exp(-z)} \tag{2.3}$$

$$\text{ReLU}(x) = max(0, x) \tag{2.4}$$

None of the previous functions can be used in the output layer of a multiclass classification problems. For this reason the *softmax* function is considered, which normalizes the output values. Then, it assigns a probability for each neuron, so that when the activation value of a neuron with respect to the others is high, it will be assigned a higher probability:

$$\text{softmax}(\mathbf{x})_j = \frac{\exp(\mathbf{x}_j)}{\sum_{i=0}^{C} \exp(\mathbf{x}_i)} \tag{2.5}$$

Parameter j corresponds to the index of output neuron. C is the size of the last layer which in classification tasks corresponds to the number of classes.

2.1.2. Loss functions

Loss function is used to compute the difference between the network prediction $\hat{y}$ and the desired prediction y. When the loss is small, it indicates that prediction is close to the expected one. There are many loss functions. Depending on the problem we want to solve one will be more recommendable than others. In this work, we will solve a sequence labelling problem. For this reason we will use cross entropy. This loss function is commonly used in classification problems.

In a binary classification problem, the output layer of a NN contains only one neuron, whose activation function is *sigmoid* (see equation 2.2). When its output is higher than a threshold, normally 0.5, the prediction will be assigned one of the categories and the other otherwise. The cross entropy loss used in that case is:

$$\mathcal{L}(\hat{y}, y) = -(y \log(\hat{y}) + (1 - y) \log(1 - \hat{y})) \tag{2.6}$$

In a multiclass classification problem, the last layer contains C neurons, where C is the total number of classes and each neuron corresponds to a different class. Also, the activation function is the *softmax* in equation 2.5; therefore, each output node will be assigned a probability. The desired prediction $y \in \mathbb{Z}^C$ is encoded using *one-hot* representation, where the value of the column associated to the class being represented is set to one and the rest to zero. Then, the output node with higher probability will

be the more promising class. The cross entropy loss used in that case is:

$$\mathcal{L}(\hat{\mathbf{y}}, \mathbf{y}) = -\sum_{i=0}^{C} y_i \log(\hat{y}_i) \tag{2.7}$$

As with *feedforward* computation (see section 2.1), where vectorization is used in order to compute the prediction for several samples in one pass, the computation of the cost is done in the same way. Therefore, the shape of the desired prediction would be $Y \in \mathbb{Z}^{C \times m}$, where m is the number of samples, and the shape of the prediction $\hat{Y}$ is the same, but being real values $\mathbb{R}$. The equation below shows that the cost function is an average loss over all samples:

$$\text{Cost}(\hat{Y}, Y) = \frac{1}{m} \sum_{i=0}^{m} \mathcal{L}(\hat{\mathbf{y}}_i, \mathbf{y}_i) \tag{2.8}$$

2.2. Training a Neural Network

Once explained the *feedforward* computation in section 2.1, where weights are involved in operations in each layer, these operations contribute to compute a final prediction $\hat{y}$, given an input data X. Ideally, whatever input data is introduced in the NN, it must always predict an output very close to the expected one. Therefore, the value of those weights are the key for a correct performance.

The weights of a *feedforward* model are initialized randomly. Common behaviour is that initial weights produce bad predictions. For this reason, the *backpropagation* algorithm [7] appeared. This algorithm adjusts the weights of the model taking into account the loss produced (see section 2.1.2). This loss will be propagated from output layer (where it is computed) until first layer (where the computation begins). The aim of the *backpropagation* algorithm is to minimize the loss. The *gradient descent* optimizer is one of the methods used by the *backpropagation* algorithm for fitting the weights W, once their respective gradients ∇ had been computed. Therefore, the chain rule is essential, in order to compute partial derivatives between the loss $\mathcal{L}$ and all weights W along the distinct neural layers that contribute to perform the prediction. The obtained gradients will be used with a *learning rate* λ for fitting the correspondent weights through *gradient descent*:

$$\triangle W = -\lambda \frac{\partial \mathcal{L}}{\partial W} \tag{2.9}$$

Nowadays, most *machine learning* (ML) frameworks automatically compute approximation of the gradients thanks to the use of automatic differentiation [29], [11].

Learning rate λ is an hyperparameter and depending on its value the effect in the networks will be different. If its value is high, local minimum would be easily avoided, since changes in the weights are higher, but it does not converge, because it will be unstable. However, with small value, learning would be slow, but it can converge better. A technique exists called *learning rate decay* where value of λ is inversely proportional to the number of training steps.

Currently, *Adam* [14] is the most popular optimizer. It computes an adaptive learning rate for each parameter. Actually, it is a combination of two previous optimizers: *gradient descent with momentum* and *RMSprop* [24]. *Gradient descent with momentum* computes the gradients using exponentially decaying average of past gradients. *RMSprop* performs the same computation but using squared gradients. *Adam* also incorporates a bias correction mechanism in order to counteract the initial steps where the bias value is close to zero.

2.2.1. Mini-batches

As seen before, vectorization is used to compute several predictions in one pass. Another important reason is that the average loss of several samples when fitting parameters allows for better generalization, thus avoiding overfitting. Overfitting happens when parameters of the model produce good performance in training set and bad ones with new data, producing the memorization of the training set. If weights are adjusted after every sample, the loss of the last samples will have higher influence in the model than the loss of the first samples.

There are three main ways of organizing samples in batches. *Stochastic gradient descent* (SGD) or *online learning* only uses one sample per batch. *Batch gradient descent*, where all samples are only in one batch; this is only useful when the number of training samples is very small. For this reason *mini-batch gradient descent* is used as usually the number of training samples is vast. This third method divides the training

samples in groups of m samples.

In *batch gradient descent* at each step the cost decreases, but in *mini-batch gradient descent* small oscillations happen at each step; this is completely normal because in each batch the set of samples is different, unlike in *batch gradient descent* in which each batch contains the same data. However, in *mini-batch gradient descent* the cost along all epochs in the training is decreasing in the similar way as occurs in *batch gradient descent*.

The most appropriate training would have all samples in one batch, but nowadays, due to the vast amount of information available, it is impracticable. For this reason, the correct option is *mini-batch gradient descent*, because SGD would require much more time, since it fits the parameters taking into account only one sample per batch instead m.

In order to reduce the cost, it is necessary to consider all training set several times; a single pass including all the samples in the training set is know as an epoch.

2.2.2. Dropout

Dropout [9] is a regularization technique that tries to avoid the overfitting of the model. This technique works by deactivating different neurons in each time step, in order to achieve better generalization. A keep probability (p_k) of each layer must be indicated.

In figure 2.3 the input layer and output layer do not use dropout, therefore all neurons in both layers are activated, but this does not happen in both hidden layers with p_k of 0.66 and 0.5 respectively. The value of non-activated neurons will be substituted by zero. For this reason in figure 2.3 no connections exist involving the deactivated neurons. Finally, the activation output of each layer will take into account the corresponding p_k:

$$\mathbf{z}^l_{\text{dropout}}[j] = \begin{cases} \frac{\mathbf{z}^l[j]}{p^l_k}, \text{ with probability } p^l_k \\ 0, \text{ with probability } 1 - p^l_k \end{cases} \tag{2.10}$$

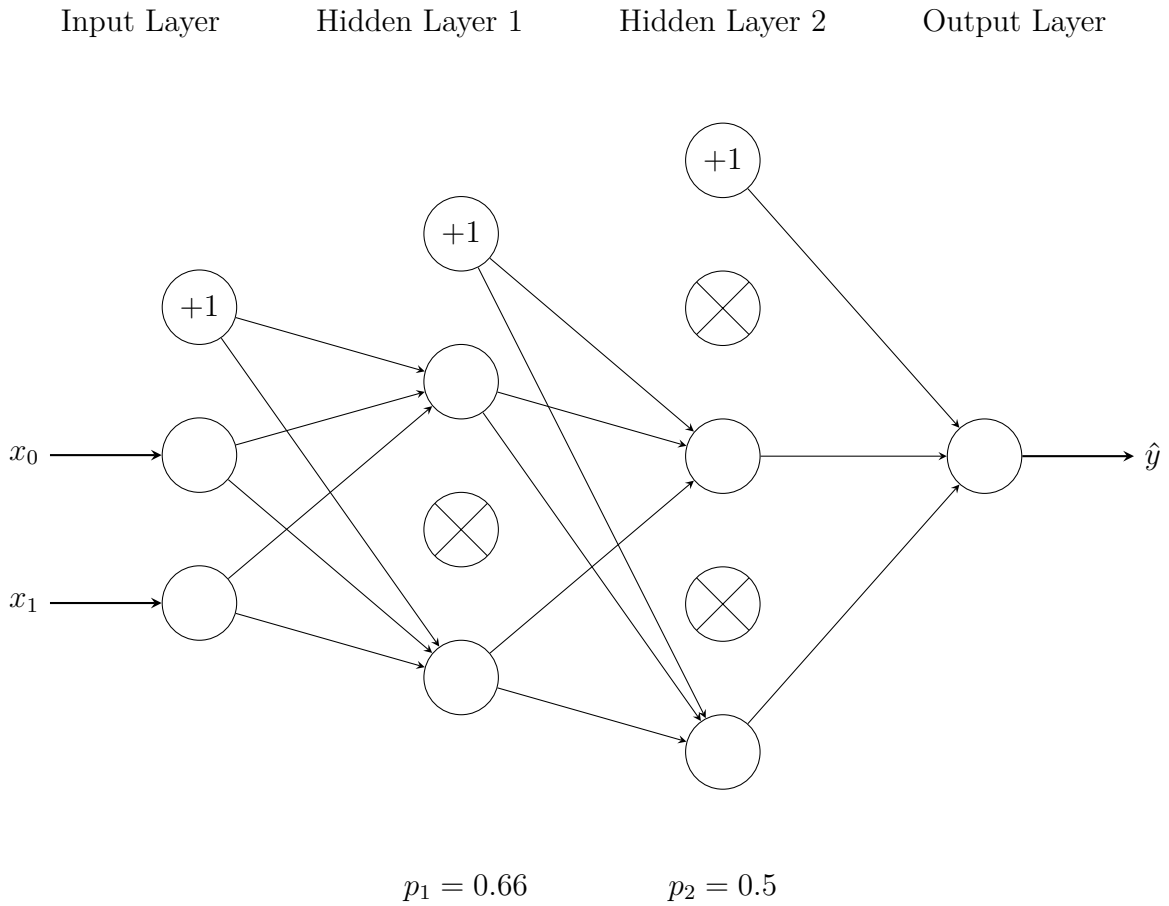

Figure 2.3: Example of a MLP with dropout.

2.2.3. Early Stopping

Early stopping [32] is another regularization technique for avoiding overfitting. It is based on using two datasets: one for training the network and another one which to decide when to stop. After each epoch of the training algorithm, the development set will be evaluated; if the cost obtained is smaller than the previous better cost obtained, that model will be saved. However, if the cost is worse in several consecutive epochs the training stops.

As can been see in figure 2.4, after epoch 400 the model is overfitting: the cost in the training set is stable, but on the development set the cost increases. For this reason, the training should be stopped at epoch 400, and the weights obtained at this epoch be used for testing.

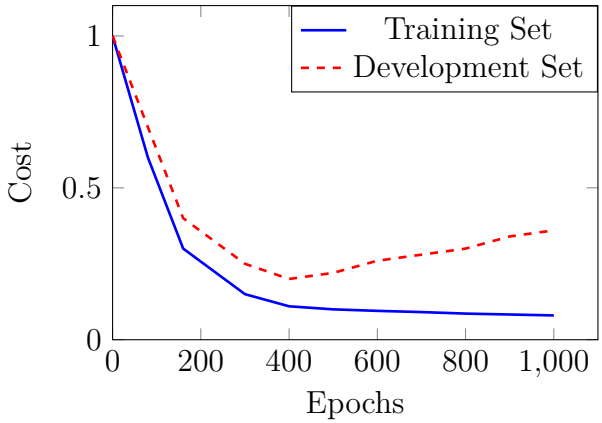

Figure 2.4: Example of early stopping.

2.3. Recurrent Neural Network

Recurrent neural network (RNN) is a neural model created for dealing with sequence data where at each time step a new input is introduced and the output for the current input may change depending on its context. This type of network has hidden states, weights and bias shared across different time steps.

Several variants of sequential information exist depending on the length of the input and output sequences. But in this work, we are only going to use many-to-many RNN where the input length T_x is the same as output length T_y, $T_x = T_y$. In addition, there exist many-to-many RNNs in which the length of the input and the output sequence are different, as in speech recognition [10] or neural machine translation [1], many-to-one as in sentiment analysis [28] or text classification [28], and one-to-many as in image captioning [20].

Figure 2.5 shows an RNN unfolded in time in which the size of the hidden estate is 3, $S = 3$. In a RNN at each time step t is computed a prediction $\mathbf{y}_t$ that corresponds to the input $\mathbf{x}_t$ fed in it. The great contribution offered by this sequence model is the use of a hidden state shared along all time steps. This hidden state $\mathbf{s}_t$ allows us to capture dependencies along time, generating different output for the same input taking the context into account. In each time step a hidden state is computed that is sent to the next time step $t + 1$.

In the first time step of equation 2.11 a previous hidden state does not exist; for this reason the initial hidden state of RNN is initialized with zeros.

This first RNN cell, computes the current hidden state $\mathbf{s}_t \in \mathbb{R}^S$ in a similar way

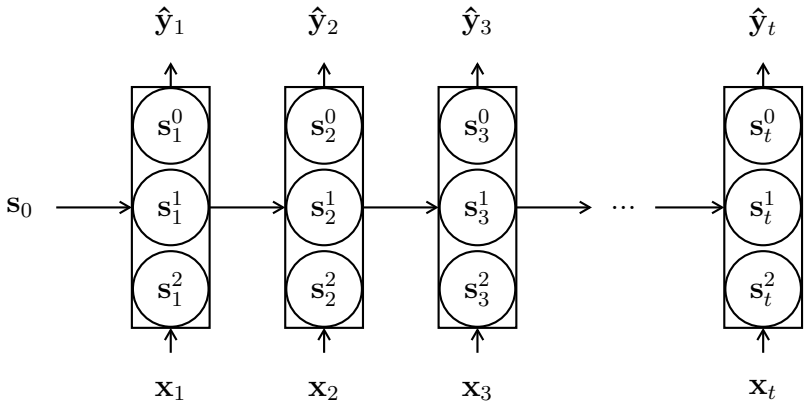

Figure 2.5: Example of an RNN unfolded in time.

to that of the NN layer (see equation 2.1), but considering two input sources instead of one, the previous hidden state $\mathbf{s}_{t-1}$ and the current input $\mathbf{x}_t \in \mathbb{R}^D$ where D is the number of the input features, therefore it uses two weights one for the current input $W_{ss} \in \mathbb{R}^{S \times S}$ and other for the previous hidden state $W_{sx} \in \mathbb{R}^{S \times D}$. After that, this current hidden state $\mathbf{s}_t$ will be used, in order to compute the current output $\hat{\mathbf{y}}_t$ in which another weights are used $W_{\hat{y}s} \in \mathbb{R}^{C \times S}$.

$$\mathbf{s}_t = \begin{cases} \mathbf{0}, & \text{if } t \text{ is } 0 \\ g(W_{ss}\mathbf{s}_{t-1} + W_{sx}\mathbf{x}_t + \mathbf{b}_s), & \text{otherwise} \end{cases} \tag{2.11}$$

$$\hat{\mathbf{y}}_t = f(W_{\hat{y}s}\mathbf{s_t} + \mathbf{b}_y) \tag{2.12}$$

As presented in section 2.2 this sequence model is trained in the same way, but more parameters to optimize exist, as can be seen in equations 2.11 and 2.12. The training algorithm used is *backpropagation through time* (BPTT) [30]. In section 2.3.1 we explain the difficulties found by this algorithm when using RNN cells [21], [3].

2.3.1. Vanishing gradient

When the last prediction $\hat{\mathbf{y}}_{T_y}$ of input sequence $\mathbf{x}$ is calculated, loss is computed. This loss is propagated backwards in time over all time steps in the RNN:

$$\frac{\partial \mathcal{L}(y_t, \hat{y}_t)}{\partial W_{t-k}} \tag{2.13}$$

W_{t-k} represents the weights of an RNN unfolded in time, where k is the number of the backward steps. When the amount of backwards steps is high, the value of the computed gradient in the weight of the corresponding time step tends to zero, therefore the contribution of it to the error is irrelevant, preventing the model from captioning long dependencies. That is very common in long sequences. This problem is known as *vanishing gradient*.

In order to solve this adversity, two neural models were proposed, first *long short term memory* (LSTM) [12] and later *gated recurrent unit* (GRU) [1] both avoiding *vanishing gradient* problem. In sections 2.3.2 and 2.3.3 respectively we will explain both models with more detail.

2.3.2. Long Short Term Memory

LSTM [12] is an extended type of neuron with the capacity to store information for a long time until it is useful. It includes a gate mechanism that forces to compute gradients whose value are very close to one, allowing a better propagation of the loss in very long sequences. In this way, it avoids the *vanishing gradient* problem and captures long distance dependencies. Therefore, the gate mechanism is a crucial improvement.

This model also includes a memory cell $\boldsymbol{c}$. The candidate memory cell $\tilde{\boldsymbol{c}}$ is computed as $\mathbf{s}_t$ (see equation 2.11) in the RNN. The gate mechanism is composed of three gates whose output values are in $[0, 1]$, allowing to maintain information through several steps or reset the memory cell, if necessary. The input gate $\mathbf{\Gamma}_i$ regulates how much the new input change the memory cell value, the forget gate $\mathbf{\Gamma}_f$ regulate how much the previous memory cell value is preserved and the output gate $\mathbf{\Gamma}_o$ regulate how much information influences the output:

$$\tilde{\mathbf{c}} = \tanh(W_{\tilde{c}s}\mathbf{s_{t-1}} + W_{\tilde{c}x}\mathbf{x}_t + \mathbf{b}_{\tilde{c}}) \tag{2.14}$$

$$\mathbf{\Gamma}_i = \sigma(W_{is}\mathbf{s_{t-1}} + W_{ix}\mathbf{x}_t + \mathbf{b}_i) \tag{2.15}$$

$$\mathbf{\Gamma}_f = \sigma(W_{fs}\mathbf{s_{t-1}} + W_{fx}\mathbf{x}_t + \mathbf{b}_f) \tag{2.16}$$

$$\mathbf{\Gamma}_o = \sigma(W_{os}\mathbf{s_{t-1}} + W_{ox}\mathbf{x}_t + \mathbf{b}_o) \tag{2.17}$$

Current memory cell $\boldsymbol{c}_t$ is influenced by the new information added to the cell and by the degree to which the previous value is deleted. For obtaining that, two element-wise multiplications are computed (Hadamard product), one between the input gate $\mathbf{\Gamma}_i$ and the candidate memory $\tilde{\boldsymbol{c}}$ (new memory) and another between the forget gate $\mathbf{\Gamma}_f$ and the previous cell memory $\boldsymbol{c}_{t-1}$ (old memory); finally both products are added:

$$\mathbf{c}_t = \mathbf{\Gamma}_u * \tilde{\mathbf{c}} + \mathbf{\Gamma}_f * \mathbf{c}_{t-1} \tag{2.18}$$

Finally, in order to compute current output $\boldsymbol{s}_t$ element-wise multiplication is used between output gate $\mathbf{\Gamma}_o$ and current memory cell value $\boldsymbol{c}_t$ which previously has been applied a tanh activation function. In this way, the output will be influenced by how much new information is added and how much old information is deleted.

$$\mathbf{s}_t = \mathbf{\Gamma}_o * \tanh(\mathbf{c}_t) \tag{2.19}$$

The prediction at current time $\hat{\mathbf{y}}_t$ is computed using a NN layer (see equation 2.1) whose input is $\boldsymbol{s}_t$.

2.3.3. Gated Recurrent Unit

Time later LSTM, GRU [1] was created. It appeared to attach the problem of *vanishing gradient* in a similar way. In this type of neuron, the current memory cell $\boldsymbol{c}_t$ and the current output $\boldsymbol{s}_t$ are the same, $\boldsymbol{c}_t = \boldsymbol{s}_t$. GRU uses two gates instead of three. These two gates are the update gate $\mathbf{\Gamma}_u$ and the reset gate $\mathbf{\Gamma}_r$. The gate mechanism and the candidate memory $\tilde{\boldsymbol{c}}$ are computed as in LSTM.

$$\tilde{\mathbf{c}} = \tanh(W_{\tilde{c}c}\mathbf{c}_{t-1} + W_{\tilde{c}x}\mathbf{x}_t + \mathbf{b}_{\tilde{c}}) \tag{2.20}$$

$$\mathbf{\Gamma}_u = \sigma(W_{uc}\mathbf{c}_{t-1} + W_{ux}\mathbf{x}_t + \mathbf{b}_u) \tag{2.21}$$

$$\mathbf{\Gamma}_r = \sigma(W_{rc}\mathbf{c}_{t-1} + W_{rx}\mathbf{x}_t + \mathbf{b}_r) \tag{2.22}$$

However, the way of computing the current memory cell is influenced by how much input information is used and how much the old memory is kept. Both multiplications are element-wise too.

$$\mathbf{c}_t = \mathbf{\Gamma}_r * \tilde{\mathbf{c}} + (1 - \mathbf{\Gamma}_u) * \mathbf{c}_{t-1} \tag{2.23}$$

This second architecture computes less operations than LSTM, for this reason it is faster in inference mode. However, in some experiment it has been shown in GRU it get worse results [8].

2.3.4. Bidirectional Recurrent Neural Networks

In many tasks, bidirectional RNNs have surpassed unidirectional performance, because posterior information may help to better predict the current output, in comparison to using only past information. Normally, one RNN is used that processes the sequence from the first element to the last one. Therefore this RNN goes forward and will be represented as $\overrightarrow{\text{RNN}}$. When the first input of the network is the last element of the sequence and the last one is the first element of the sequence, this second RNN goes backward and will be represented as $\overleftarrow{\text{RNN}}$.

A bidirectional RNN is composed by two RNNs as can be seen in figure 2.6. Each RNN processes the input in a different direction. The output of both RNN generated at each time step are concatenated $[\overrightarrow{\mathbf{s}_t}, \overleftarrow{\mathbf{s}_t}]$ and this is the prediction of the bidirectional RNN:

$$\hat{\mathbf{y}}_t = g(W_y[\overrightarrow{\mathbf{s}_t}, \overleftarrow{\mathbf{s}_t}] + \mathbf{b}_y) \tag{2.24}$$

2.3.5. Stacked Recurrent Neural Networks

Several problems exists whose complexity is very high like *machine translation* in the NLP field. Architectures with only one layer can not get a good performance. For this reason it is necessary to increment the number of layers in order to learn more abstract features. Figure 2.7 shows a RNN with three stacked layers.

In the first layer, the input at each time step is the corresponding element of the input sequence $\mathbf{x}_t$, but in the remaining layers, the input is the hidden state of the

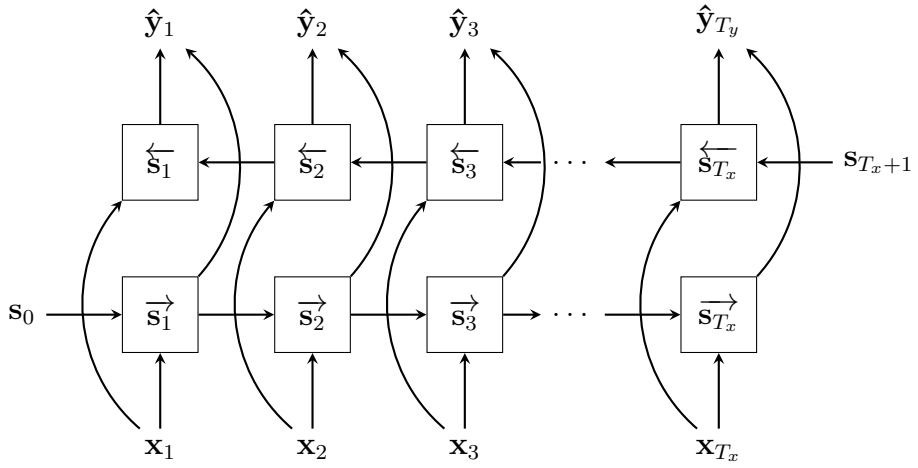

Figure 2.6: Example of a bidirectional RNN.

previous layer at the same time step $\mathbf{s}_t^{l-1}$; obviously, the previous hidden state belongs to the same layer l $\mathbf{s}_{t-1}^l$:

$$\mathbf{s}_t^l = g(W_{ss}^l \mathbf{s}_{t-1}^l + W_{sx}^l \mathbf{s}_t^{l-1} + \mathbf{b}_s^l) \tag{2.25}$$

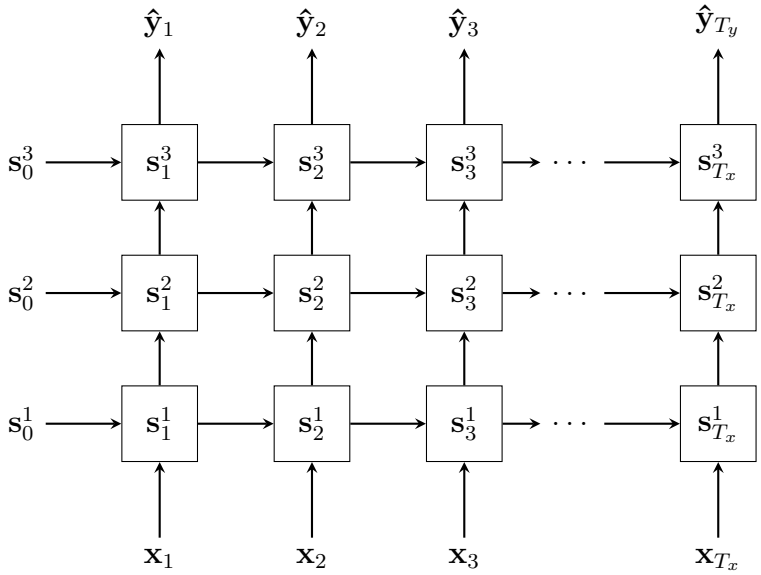

Figure 2.7: Example of an unidirectional RNN with 3 stacked layers.

2.3.6. Variable Sequence Lengths

In all human languages the lengths of the sentences are different. As has been explained in the previous sections, in order to attain fast computations it is crucial to follow vectorization methods, and therefore we must group sequences in mini-batches

(see section 2.2.1). Since sequences have different length, it is necessary to pad all sequences to have the same length. This length would be the maximum length existing in the corresponding mini-batch. Padding a sequence consists in adding a pad token `<pad>` to the end of the original sequence, until this padded sequence gets the expected length:

$$\mathbf{x}_0 = \begin{bmatrix} x_0^0 & x_1^0 \end{bmatrix}; \quad \mathbf{x}_1 = \begin{bmatrix} x_0^1 & x_1^1 & x_2^1 \end{bmatrix}; \quad X = \begin{bmatrix} x_0^0 & x_1^0 & \texttt{<pad>} \\ x_0^1 & x_1^1 & x_2^1 \end{bmatrix}$$

However, in order to compute the actual loss $\mathcal{L}_{actual}$ of the mini-batch, the loss of the padded tokens has to be omitted. For doing that, a mask $\mathcal{M}$ is used with the same shape of the mini-batch input where zero elements correspond with padded elements:

$$\mathcal{M} = \begin{bmatrix} 1 & 1 & 0 \\ 1 & 1 & 1 \end{bmatrix}$$

The padded input X is introduced in a sequence model like RNN, generating a prediction $\hat{Y}$:

$$\hat{Y} = \text{RNN}(X);$$

The total loss $\mathcal{L}_{total}$ is computed between the prediction of the RNN and the desired prediction Y. After that, element-wise multiplication between the total loss and the mask is computed in order to obtain the actual loss:

$$\mathcal{L}_{total} = \mathcal{L}(\hat{Y}, Y) = \begin{bmatrix} \mathcal{L}_0^0 & \mathcal{L}_1^0 & \mathcal{L}_2^0 \\ \mathcal{L}_0^1 & \mathcal{L}_1^1 & \mathcal{L}_2^1 \end{bmatrix}; \quad \mathcal{L}_{actual} = \mathcal{L}_{total} * \mathcal{M} = \begin{bmatrix} \mathcal{L}_0^0 & \mathcal{L}_1^0 & 0 \\ \mathcal{L}_0^1 & \mathcal{L}_1^1 & \mathcal{L}_2^1 \end{bmatrix}$$

2.3.7. Sequence to sequence

Sequence to sequence (Seq2Seq) [26] is an encoder-decoder architecture, where input sequence is encoded by an RNN, whose hidden state in the last time step is used as the initial state of an RNN decoder. The decoder predicts the current output $\hat{\mathbf{y}}_t$ given the previous one $\hat{\mathbf{y}}_{t-1}$ and the hidden state. As it does not exist a previous element for the

first prediction, an initial and end element are created for all sequences. Therefore, all output sequences share an initial element `<sos>` that means beginning of the sequence and is the first input introduced in the decoder, and also they share an end element `<eos>` too, that is the last element that must be predicted by the decoder. This architecture allows to tackle problems in which the input and output sequences have different length. Because of that, all elements produced by the decoder that appear after the end element are ignored.

Figure 2.8 shows a Seq2Seq where input sequence size is three and output is four, without taking into account the `<sos>` and `<eos>` elements.

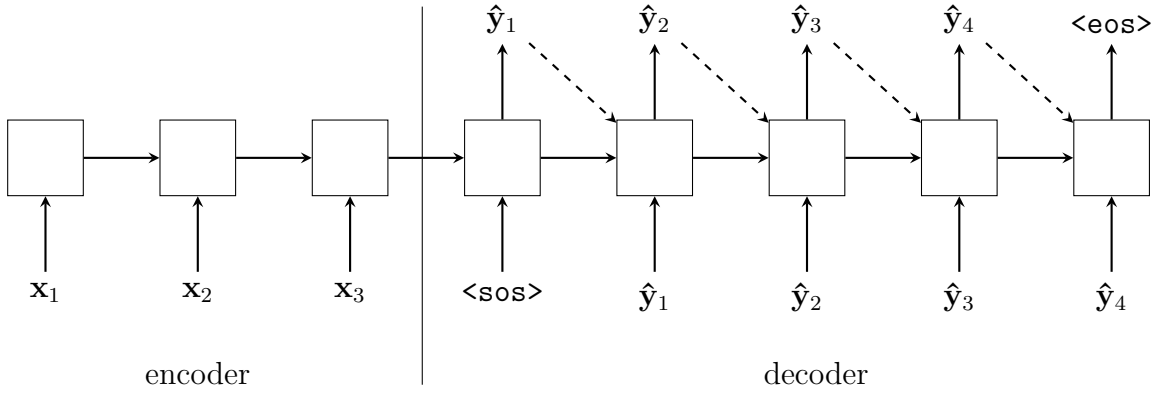

Figure 2.8: Example of a Seq2Seq architecture.

2.3.8. Beam Search

As already discussed in section 2.3.7, the decoder predicts the current output $\hat{\mathbf{y}}_t$ given the previous one $\hat{\mathbf{y}}_{t-1}$ and the hidden state. Therefore, at each time step the network is fed with the more promising class; this is known as the *greedy search* approach to decoding. The score of an output sequence is the product of all the element probabilities. Therefore, the first element predicted with high probability does not necessarily belong to the output sentence with the highest score. For this reason the *beam search* technique [31] appeared, where n most promising classes are taken at each step, generating n different output sequences instead of one as occurs with the *greedy search* approach. Also, it is important to take into account the length of the sequence in order to choose the most promising sequence, because normally a long sequence has smaller probability than a shorter one, but a longer one could be a better output

sequence. In order to overcome this issue, the score is normalized taking into account the length of the predicted output too.

Figure 2.9 shows a *beam search* with a beam width of 2, where the most promising output sequence (BS) is not the expected output produced by the *greedy search* approach (G).

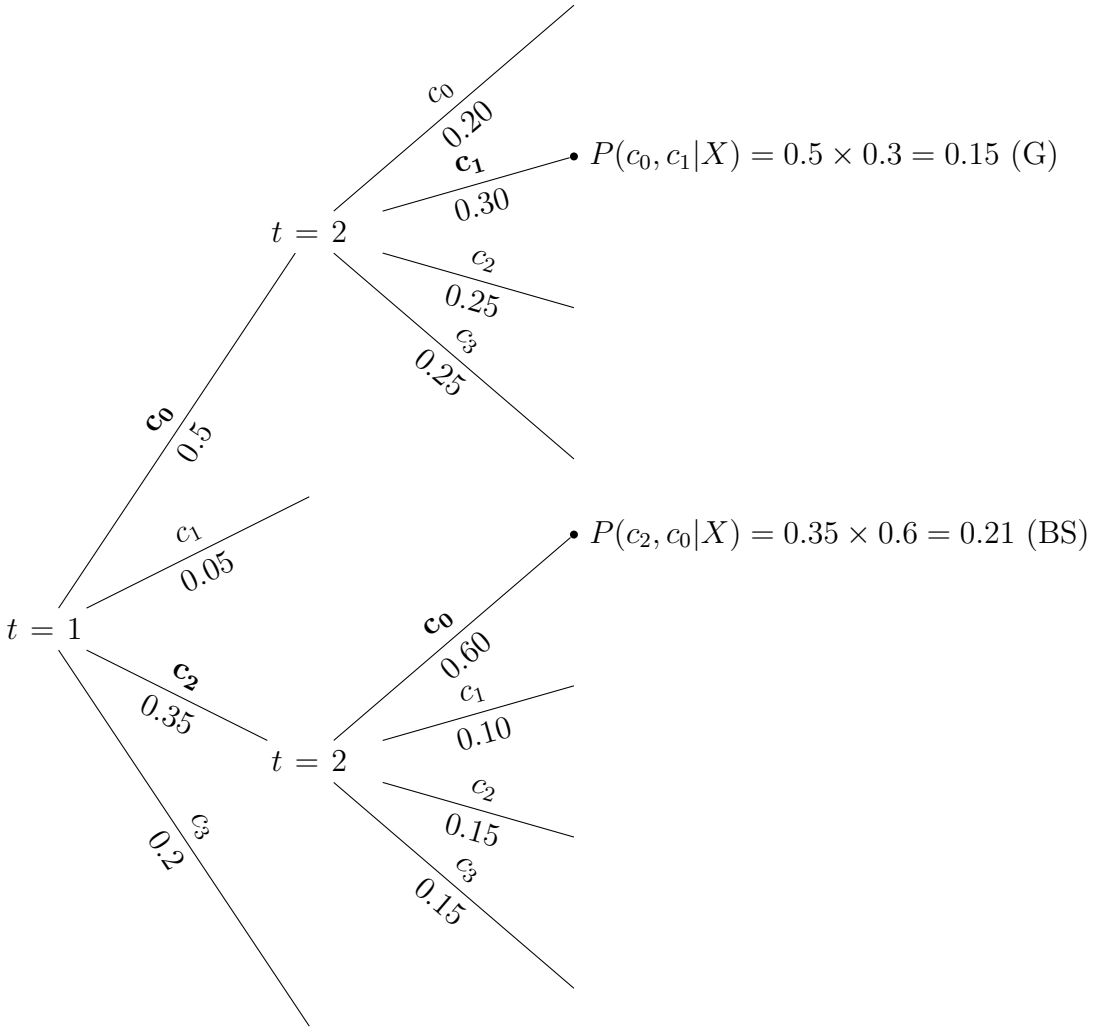

Figure 2.9: Example of a beam search with beam width of 2.

2.3.9. Attention

The problem of Seq2Seq (see section 2.3.7) is that it uses a fixed encoded state for the whole source sequence, and it is very difficult to compress all meaning of the source sentence into a single vector. Attention [2] appeared to overcome this issue. This mechanism generates at each decoding time step a different encoded representation **c** (context) of the source sequence. For doing that, it requires to store all the hidden

states $\mathbf{h}_i$ generated by the encoder.

$$a(\mathbf{s}_{t-1}, \mathbf{h}_j) = f(W_{as}\mathbf{s}_{t-1} + W_{ah}\mathbf{h}_j + \mathbf{b}_a) \tag{2.26}$$

$$\alpha_{ij} = \frac{\exp(a(\mathbf{s}_{i-1}, \mathbf{h}_j))}{\sum_{k=0}^{T_x} \exp(a(\mathbf{s}_{i-1}, \mathbf{h}_k))} \tag{2.27}$$

$$\mathbf{c}_i = \sum_{j=0}^{T_x} \alpha_{ij}\mathbf{h}_j \tag{2.28}$$

Equation 2.26 computes the degree of attention between one element of input sequence $\mathbf{x}_j$ and next element of the output sequence $\hat{\mathbf{y}}_t$. For doing so it uses a NN layer between the corresponding hidden state of the encoder $\mathbf{h}_j$ and the previous hidden state of the decoder $\mathbf{s}_{t-1}$. This computation will be performed for all hidden states of the input sequence. Then, equation 2.27 computes a scalar value α_{ij} (energy) for each value obtained in equation 2.26; this value indicates how much attention has to be put into $\mathbf{x}_j$ to predict $\hat{\mathbf{y}}_i$. Finally, variable encoded state is computed in equation 2.28, by simply performing a weighted sum of attention states with the corresponding energy values.

Figure 2.10 uses an input and output sequence generated by the automaton shown in figure 5.4. This automaton contains backward and forward dependencies; therefore, the attention matrix shows an output that requires backward dependencies to predict it correctly like c_2 at t_3 where it has to put attention into the corresponding current input a_2 and the corresponding previous one a_0, and the same happens with c_4 at t_5 but requiring forward dependencies. The remaining outputs only require focusing on the corresponding current input to predict them correctly.

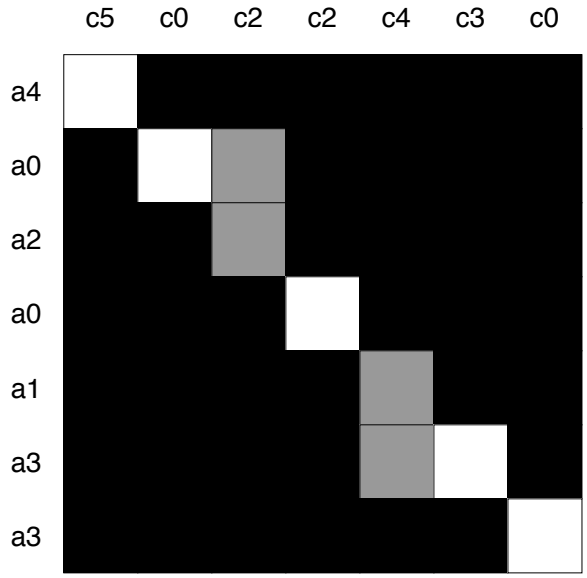

Figure 2.10: Example of an attention matrix.

Chapter 3

Material and Methods

3.1. Introduction

In a DL project there are three resources that are necessary to finish it with success. The first one is related to programming. We need to code complex neural networks easily and reduce as much as possible the time needed to code them and the likelihood of bugs. For this reason, the best option is choosing an open source specialized *machine learning* (ML) framework, such as TensorFlow (see section 3.2). The second one is data. It is advisable to use publicly available datasets in order to ensure reproducibility and make it easier the comparison with state-of-the-art approaches. In this way, it will be easy to compare them with our own results. The last one is related to the equipment used for training the models. Training deep neural networks requires dedicated hardware (GPUs) which if it is not available makes training very time consuming, which may prevent testing different configurations.

3.2. Framework

Thanks to the DL boom, many open source frameworks specialized in ML like CNTK[1], PyTorch[2], Keras[3] and TensorFlow[4] have appeared.

Prior to the development of this project, I had coded some NN toy models in Keras, and I had to understand the computation graph of TensorFlow, which is the framework

[1] https://www.microsoft.com/en-us/cognitive-toolkit/
[2] https://pytorch.org
[3] https://keras.io
[4] https://www.tensorflow.org

internally used by Keras. In this project I have gone deeper in understanding and programming NN in TensorFlow.

3.2.1. TensorFlow

TensorFlow [18] is an open-source library for numerical computation which uses data flow graphs. It is developed by Google Brain starting in 2015. The initial aim of this library was to encourage research in ML. The software developed with this library is easily deployed in a variety of hardware platforms like CPUs, GPUs and mobile devices, among others.

In this project, the main learning objective is to acquire the knowledge to develop NN models working with sequences of variable length, like natural language sentences. TensorFlow provides tf.data[5] which allows to easily preprocess a dataset composed of variable-length sequences and tf.contrib.rnn[6] which prototypes RNN in a simple way. TensorFlow also incorporates tf.contrib.seq2seq[7] [8], which allows the development of Seq2Seq architectures with attention mechanism and beam search. For this reasons, TensorFlow is ideal for this work.

3.3. Dataset

There are many PoS tagging datasets available, like the Brown[8] corpus; however, there is one corpus that may be considered the standard dataset because it is used in most relevant research on part-of-speech tagging[9]. That dataset is the Penn Treebank [17].

3.3.1. Penn Treebank - Wall Street Journal

The Wall Street Journal (WSJ): WSJ is a collection of English news; is a portion of the Penn Treebank composed of 25 sections (0-24). This dataset contains 45 PoS tags, of which 36 are lexical categories[10] and the rest are punctuation marks. Tables

[5] https://www.tensorflow.org/api_docs/python/tf/data
[6] https://www.tensorflow.org/api_docs/python/tf/contrib/rnn
[7] https://www.tensorflow.org/api_docs/python/tf/contrib/seq2seq
[8] http://www.hit.uib.no/icame/brown/bcm.html
[9] https://nlpprogress.com/english/part-of-speech_tagging.html
[10] https://www.ling.upenn.edu/courses/Fall_2003/ling001/penn_treebank_pos.html

3.1 and 3.2 show the PoS tag used in the WSJ dataset.

Tag	Description	Tag	Description
CC	Coordinating conjunction	CD	Cardinal number
DT	Determiner	EX	Existential there
IN	Preposition or subordinating conjunction	FW	Foreign word
JJ	Adjective	JJR	Adjective, comparative
JJS	Adjective, superlative	LS	List item marker
MD	Modal	NN	Noun, singular or mass
NNS	Noun, plural	NNP	Proper noun, singular
NNPS	Proper noun, plural	PDT	Predeterminer
POS	Possessive ending	PRP	Personal pronoun
PRP$	Possessive pronoun	RB	Adverb
RBR	Adverb, comparative	RBS	Adverb, superlative
RP	Particle	SYM	Symbol
VBZ	Verb, 3rd person singular present	UH	Interjection
VB	Verb, base form	VBD	Verb, past tense
VBG	Verb, gerund or present participle	VBN	Verb, past participle
VBP	Verb, non-3rd person singular present	TO	to
WDT	Wh-determiner	WP	Wh-pronoun
WP$	Possessive wh-pronoun	WRB	Wh-adverb

Table 3.1: PoS tag in the WSJ dataset corresponding to lexical categories.

Tag		
,	(	$
)	.	#
:	“	’

Table 3.2: PoS tags in the WSJ dataset corresponding to punctuation marks.

3.4. Equipment

We use the Compute Engine[11] service of Google Cloud Platform (GCP) for training our neural models. Table 3.3 shows the characteristic of the computing instance used. In order to be able to run TensorFlow in graphics processing units (GPU) it is mandatory to have installed the *CUDA Deep Neural Network Library* (cuDNN) with the *Compute Unified Device Architecture* (CUDA) driver. Therefore, I had to install the software listed in table 3.4.

[11] https://cloud.google.com/compute/

Natural language toolkit (NLTK) will be used to tokenize the corpora. Each word will be substituted by the correspondent ambiguity class which will be the input to the neural network.

Computing Instance	
OS	Ubuntu 16.04 LTS
SSD	50 GB
RAM	30 GB
CPU's cores	16
GPU	Tesla P100-PCIE-16GB

Table 3.3: Characteristics of the GCP instance used.

Package	**Version**
Python	3.5
CUDA	9.0
cuDNN	7.2
TensorFlow	1.10.1
NLTK	3.3.0

Table 3.4: Software requeriments.

Chapter 4

Architectures

This fourth chapter shows the way of encoding ambiguity classes (see section 4.1) as input to the NN models and describes the NN architectures we have explored (see section 4.2) to tackle the problem described in chapter 1.

4.1. Encode ambiguity classes

In this work we represent the ambiguity classes (see section 1.2) in two different ways. The first one uses *one-hot* encoding where each ambiguity class identifier is substituted by a vector $\mathbf{X^o} \in \mathbb{Z}^A$ where A is the size of the set of ambiguity classes and the element of the column associated to the ambiguity class being represented is set to one and the rest to zero. The second one uses *multi-hot* encoding where an ambiguity class is represented by a vector $\mathbf{X^m} \in \mathbb{Z}^C$ where C is the size of the tagset and the value of the columns columns associated to the tags in the ambiguity class being represented are set to one, and to zero otherwise. *Multi-hot* offers a more compact representation of the ambiguity classes than *one-hot* and also allows to incorporate new words belonging to ambiguity classes not seen in the training corpus.

Table 4.1 shows PoS tags that belongs to each ambiguity class in the automaton of figure 5.4. In this example the number of ambiguity classes is 6 and the size of the tagset is 7. Therefore, the *one-hot* representation of the ambiguity class a_3 would be: $[0, 0, 0, 1, 0, 0]$; and its *multi-hot* representation would be: $[1, 0, 0, 1, 0, 0, 0]$.

	c_0	c_1	c_2	c_3	c_4	c_5	.
a_0	X		X				
a_1		X			X		
a_2			X	X			
a_3	X			X			
a_4						X	
a_5							X

Table 4.1: Relation between ambiguity class (rows) and PoS tags (columns).

4.2. Architectures

We propose to evaluate three NN architectures for our PoS task: the first one uses RNN (see section 4.2.1); the second one is an architecture in two phases that uses RNN in the first phase and *feedforward* NN in the second phase [22] (see section 4.2.2); the third one is a Seq2Seq architecture with attention mechanism (see section 4.2.3).

4.2.1. RNN Architecture

Figure 4.1 shows the RNN architecture. The input to the RNN is a sequence of *multi-hot* representation of ambiguity classes $\mathbf{X^m}$. The output value of the RNN $\mathbf{h}$ (see section 2.3) is introduced to a NN layer (see equation 2.1). The values used to compute the cross entropy loss (see section 2.3.6) are the expected PoS tag $\mathbf{y}$ and the output value of the NN layer $\mathbf{s}$ in which a softmax function is applied, assigning a probability to each PoS tag $\hat{\mathbf{y}}$; therefore the PoS tag with the greatest probability, it will be the most promising PoS tag and the prediction of the network to tag the word.

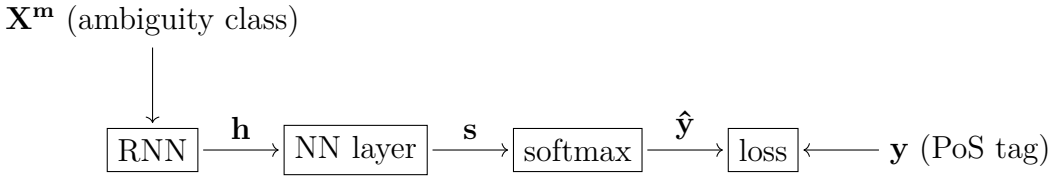

Figure 4.1: RNN architecture.

4.2.2. Architecture in two phases

The second architecture, shown in figure 4.2, learns two tasks. The first task consist of predicting the next ambiguity class using a RNN. The input to this phase is a sequence of *one-hot* representations of ambiguity classes $\mathbf{X^o}$. The output value of the

RNN $\mathbf{h}$ is introduced to a NN layer, generating the output value of the first phase $\mathbf{s}$. The second task predicts the PoS tag using a *feedforward* NN and the input of this phase is $\mathbf{h}$. In this way, the first task provides context information to the second one.

We propose training this architecture in two phases [22]. The first one minimizes the loss of predicting the next ambiguity class; computing the cross entropy loss (see section 2.3.6) between the output of the first phase in which softmax_1 is applied, assigning a probability to each ambiguity class $\hat{\mathbf{y}}_1$ and the expected next ambiguity class $\mathbf{y_1}$. Once this task converges, it is time to train the second one by minimizing the loss of predicting the PoS tag, computing the cross entropy loss between the output of the second phase that is the output of the *feedforward* NN $\mathbf{z}$ in which softmax_2 is applied, assigning a probability to each PoS tag $\hat{\mathbf{y}}_2$ and the expected PoS tag $\mathbf{y_2}$. It is worth nothing that, in the second phase the loss is propagated to the parameters used in the first phase as well. This is done because those parameters contribute to the final prediction.

The greatest probability of $\hat{\mathbf{y}}_1$ will be the most promising ambiguity class and prediction of the network in the first phase. The same happens with $\hat{\mathbf{y}}_2$ whose greatest probability will be the most promising PoS tag and the prediction of the network in the second phase.

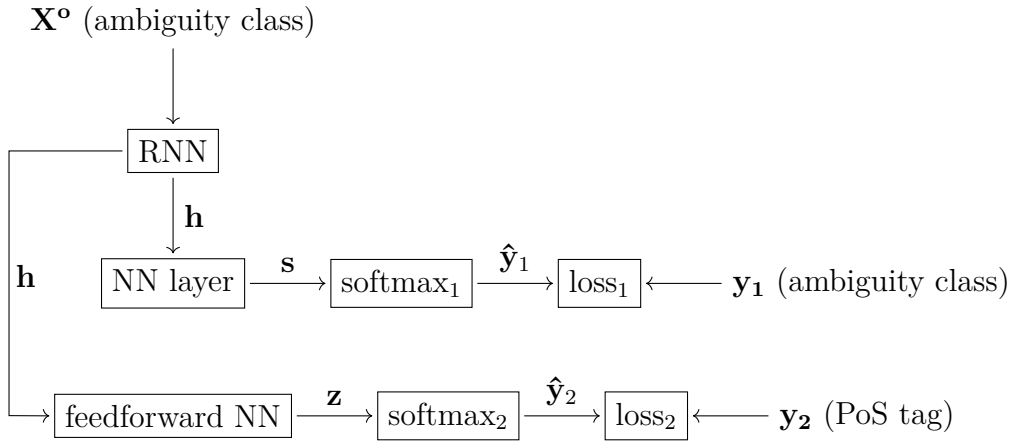

Figure 4.2: Architecture in two phases.

4.2.3. Seq2Seq with Attention Architecture

The last architecture, a Seq2Seq with attention mechanism, is shown in figure 4.3. The input to the Seq2Seq is a sequence of *multi-hot* representation of ambiguity classes $\mathbf{X^m}$. The output value of the Seq2Seq with attention mechanism $\hat{\mathbf{y}}$ (see sections 2.3.7

and 2.3.9) and the expected PoS tag $\mathbf{y}$ are used to compute the cross entropy loss (see section 2.3.6). The PoS tag with the greatest probability $\hat{\mathbf{y}}$, it will be the most promising PoS tag and the prediction of the network..

The encoder of the Seq2Seq provides context information to the decoder of the Seq2Seq, as it happens in the architecture in two phases (see section 4.2.2) in which the first phase provides context information to the second phase. Also, the input of this architecture is influenced by RNN architecture (see section 4.2.1), because it uses *multi-hot* representation of ambiguity classes as input instead of *one-hot* representation. For these reasons, this architecture combines the two previous architectures.

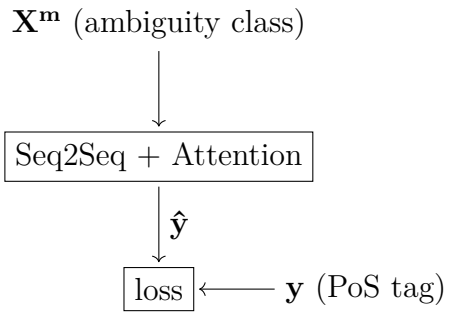

Figure 4.3: Seq2Seq with attention architecture.

Chapter 5

Experiments

In this fifth chapter we explain the naive baselines (see section 5.1). Next, we present the synthetic dataset (see section 5.2). Finally, we show the results of the experiments with the synthetic (see section 5.2.5) and the Wall Street Journal (see section 5.3.1) datasets. Also, the open source implementation of this Bachelor's Thesis is available online in *GitHub* [1] in order to ensure that all the experiments can be reproduced.

5.1. Naive baselines

We compare the performance of our approaches against three naive baselines: one working at the PoS tag level (see section 5.1.1), a second one working at the ambiguity level (see section 5.1.2) and a third one working at the word level (see section 5.1.3). They are based on counting PoS tags. The ambiguity class for unknown words counts all the PoS tags in the training corpus and chooses the PoS tag that belongs to the open lexical categories (see section 1.2) with the highest number of occurrences.

5.1.1. Tag level

This first naive baseline counts the number of occurrences of each PoS tag in the training set, and then, given an ambiguity class; chooses the PoS tag that belongs to that ambiguity class with a higher number of occurrences in the training corpus.

[1] https://github.com/franborjavalero/npostagging

5.1.2. Ambiguity level

This second naive baseline counts the number of occurrences of each PoS tag associated with each ambiguity class in the training set, and then, given an ambiguity class chooses its PoS tag with a higher number of occurrences in the training corpus.

5.1.3. Word level

This third naive baseline counts the number of occurrences of each PoS tag associated with each word in the training set, and then, given a word chooses its PoS tag with a higher number of occurrences in the training corpus.

5.2. Synthetic dataset

Our approach to PoS tagging predicts a PoS tag given an ambiguity class (see section 1.2). Depending on the context, this PoS tag may change. For better understanding the problem, we have built different automata emulating the behaviour of the natural language in different scenarios. These small automata are then joint together (see section 5.2.4) to create synthetic data.

The three small automata, we have built are: one with backward dependencies (see section 5.2.1), a second one with forward dependencies (see section 5.2.2) and a third one without dependencies (see section 5.2.3).

5.2.1. Automaton with backward dependencies

Figure 5.1 shows the automaton with backwards dependencies. At time step t, the tagger has to assign a PoS tag to ambiguity class a_2, but this ambiguity class is ambiguous, as it can be assigned the PoS tag c_2 or c_3. In this scenario, it is crucial to know the ambiguity class at the previous time step $t-1$ in order to correctly predict the PoS tag of ambiguity class a_2. If the previous ambiguity class is a_1, the current PoS tag assigned to a_2 must be c_3; otherwise, the previous ambiguity class is a_0, and the tagger must assign to a_2 the PoS tag c_2. This automaton generates an input sequence that is constituted by ambiguity classes and its corresponding output sequence that is constituted by PoS tags. For instance, the input sequence $[a_0, a_2]$ its corresponding

output sequence is $[c_0, c_2]$.

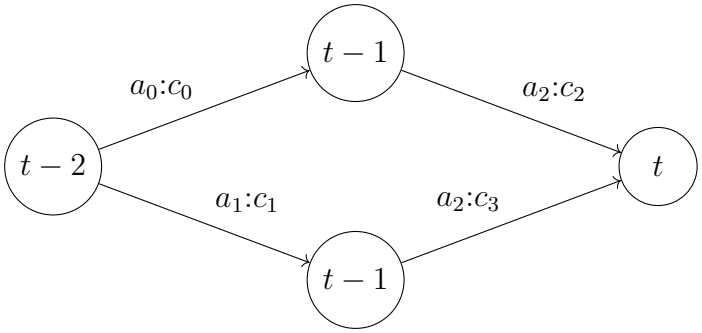

Figure 5.1: Automaton with backward dependencies.

5.2.2. Automaton with forward dependencies

Figure 5.2 shows the automaton with forward dependencies. It is very similar to the one in figure 5.1, but in the opposite direction, that is, for predicting correctly the PoS tag of ambiguity class a_0 it is necessary to know the ambiguity class in subsequent time step $t+1$. If in $t+1$ the ambiguity class is a_1, the current tag must be c_0; otherwise, when the subsequent ambiguity class is a_2, the current tag must be c_1.

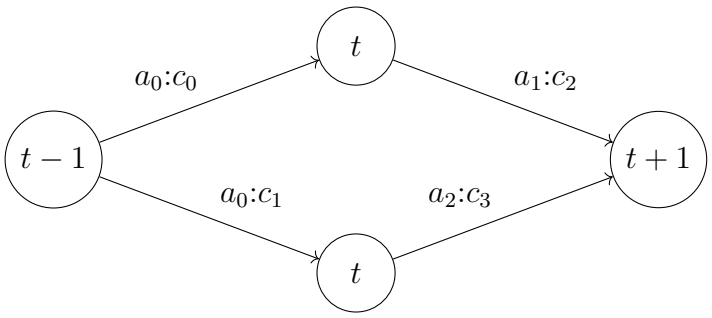

Figure 5.2: Automaton with forward dependencies.

5.2.3. Automaton without dependencies

Figure 5.3 shows the automaton without dependencies. This automaton does not have to take into account backward and forward dependencies, therefore at time step t, the tagger has to assign PoS tag c to ambiguity class a.

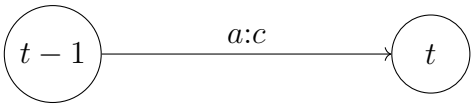

Figure 5.3: Automaton without dependencies.

5.2.4. Complex automaton

The three simple automata described in previous sections (5.2.1, 5.2.2 and 5.2.3) can be combined in different ways to obtain a complex automaton (see figure 5.4). This complex automaton can be considered as a simplification of the real problem that we want to tackle. This automaton generates 4 different input sequences with their corresponding output sequences, also it contains 2 states that can take two different ways with the same probability.

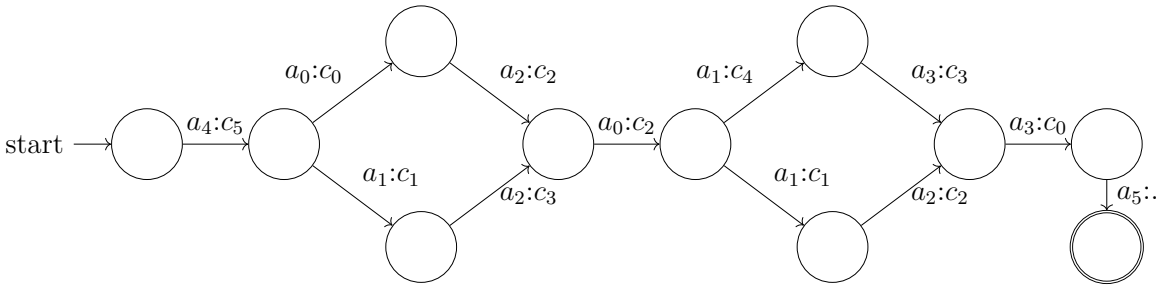

Figure 5.4: Toy language automata.

5.2.5. Results

We use the complex automaton shown in figure 5.4 to ensure that our NN architectures learn from toy data. In these experiments, training, development and test sets contain the same 4 input and output sequences generated by the automaton, but with different distributions. These sets consist of 20,000, 200 and 200 sequences, respectively, chosen at random. Table 5.1 shows the NN setup used for training the models with synthetic data.

In all the experiments of this work, the accuracy is a score in [0,1] that indicates the correct predictions and the cost is computed using the equation 2.8. Figure 5.5 shows the results of the architecture in two phases (listed in table 5.1) predicting the next ambiguity class during the training. As can see in figure 5.5, the unidirectional RNN can not learn perfectly the input sequences generated by the automata, because it only takes into account backwards dependencies, for this reason bidirectional RNN learns

Architectures								
RNN	**Type**	**Layers**	**Units**	**Model name**				
	LSTM	1	8	lstm8				
	Bi-LSTM			blstm8				
Two phases	**Phase 1: RNN**			**Phase 2: feedforward NN**		**Model name**		
	Type	**Layers**	**Units**	**Hidden layers**	**Units**			
	LSTM	1	8	1	8	lstm8-nn8		
	Bi-LSTM					blstm8-nn8		
Seq2Seq	**Encoder**			**Decoder**			**Attention**	**Model name**
	Type	**Layers**	**Units**	**Type**	**Layers**	**Units**	**Units**	
	LSTM	1	8	LSTM	1	8	8	lstm8-lstm8-a8
	Bi-LSTM							blstm8-lstm8-a8

Table 5.1: NN setup used with the synthetic dataset.

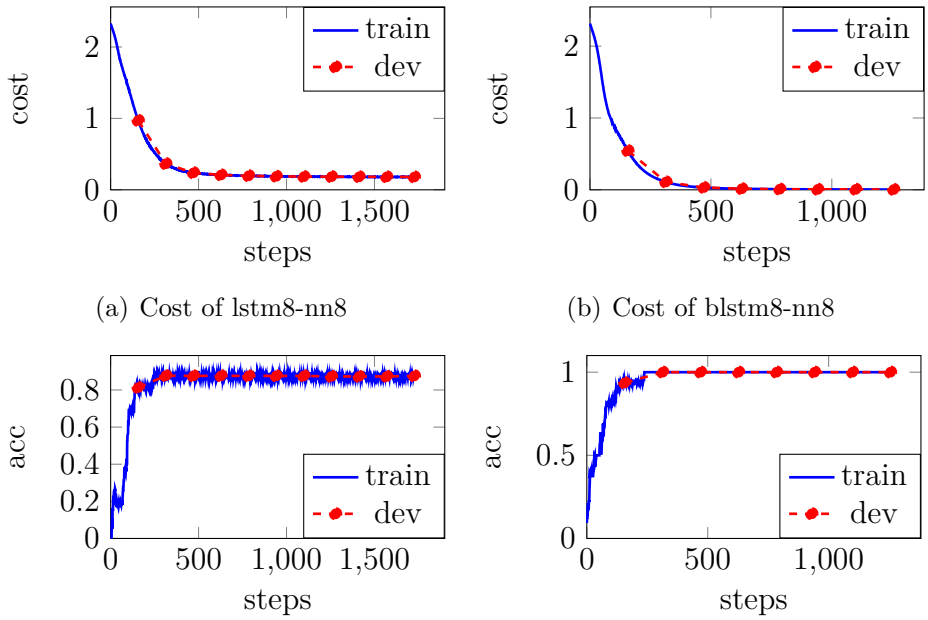

(a) Cost of lstm8-nn8

(b) Cost of blstm8-nn8

(c) Accuracy of lstm8-nn8

(d) Accuracy of blstm8-nn8

Figure 5.5: Results of the architecture in two phases predicting the next ambiguity class using the synthetic dataset.

perfectly the input sequences generated by the automata, because it takes into account backwards and forwards dependencies. Table 5.2 shows the result in inference mode of predicting the next ambiguity class too, but once finished the training of predicting PoS tag. As can see in figure 5.5 and in table 5.2, the results do not match. This happens, because the weights of the second phase fit the weights of the RNN in order to minimize the loss of predicting PoS tag, producing worse predictions for predicting the next ambiguity class.

Figures 5.6, 5.7 and 5.8 show the values of the cost and the accuracy obtained for all the models (listed in table 5.1) during training of predicting PoS tag. Table 5.3 shows results on the test set. In the toy automaton language shown in figure

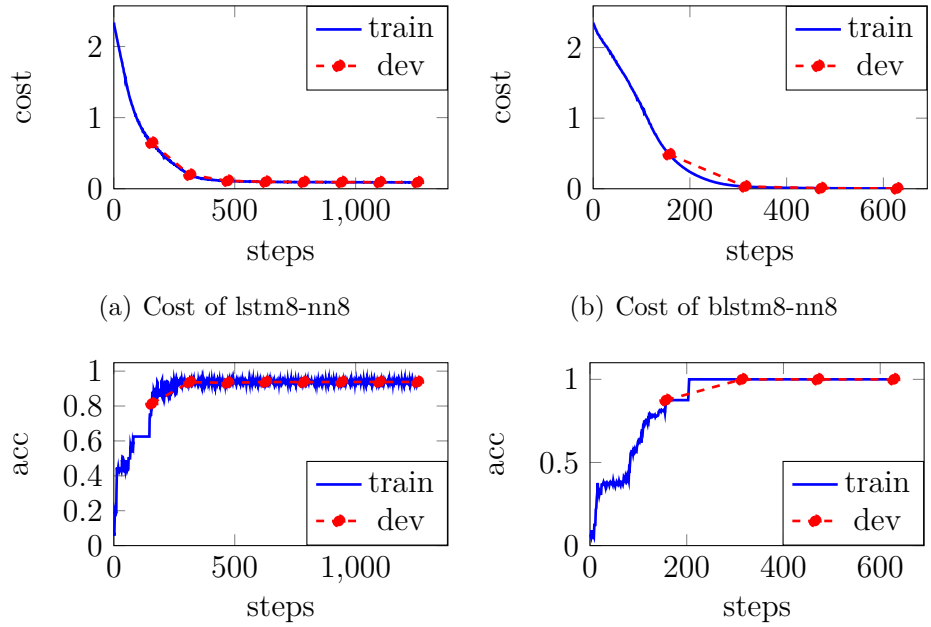

(a) Cost of lstm8-nn8

(b) Cost of blstm8-nn8

(c) Accuracy of lstm8-nn8

(d) Accuracy of blstm8-nn8

Figure 5.6: Results of the architecture in two phases predicting PoS tag using the synthetic dataset.

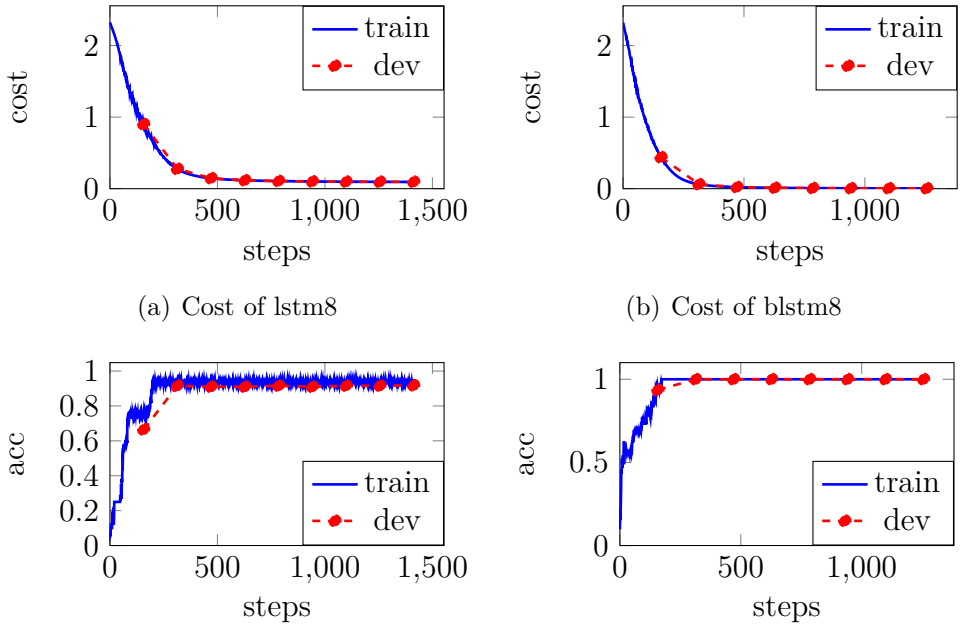

(a) Cost of lstm8

(b) Cost of blstm8

(c) Accuracy of lstm8

(d) Accuracy of blstm8

Figure 5.7: Results of the RNN architecture on the synthetic dataset.

5.4, the three naive baselines produce the same accuracy values, because each word correspond with a different ambiguity class, therefore there are not more than one word that belongs to the same ambiguity class. These results confirm bidirectional surpass unidirectional in this type of problem, because data contains forward dependencies

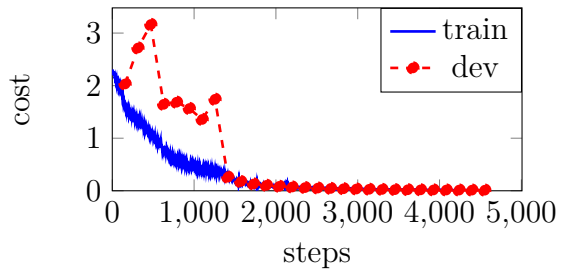

(a) Cost of seq8-seq8-a8

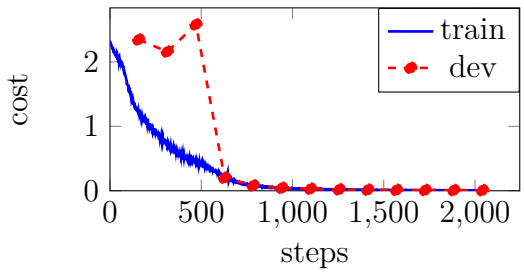

(b) Cost of bseq8-seq8-a8

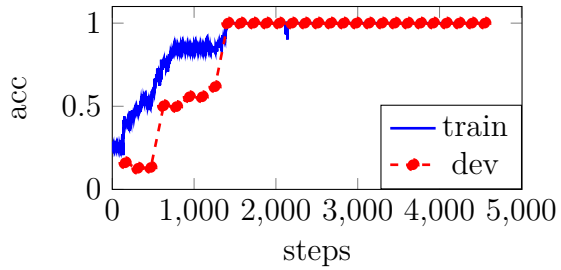

(c) Accuracy of seq8-seq8-a8

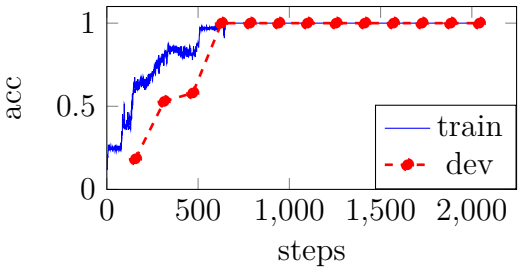

(d) Accuracy of bseq8-seq8-a8

Figure 5.8: Results of the Seq2seq architecture on the synthetic dataset.

too, not only backward dependencies. For this reason, in WSJ experiments we will use only bidirectional. However, in the Seq2Seq architecture with an unidirectional RNN encoder learns perfectly the prediction of PoS tag, because in this simple toy automata language with the variable encoded estate computed by the attention mechanism and the prediction in the previous time step are sufficient to predict correctly the PoS tag. Later, we will see if it happens the same with WSJ dataset.

Model	**Cost**	**Accuracy**
lstm8-nn8	1.146	0.681
blstm8-nn8	0.226	0.856

Table 5.2: Results of predicting the next ambiguity class with the synthetic dataset.

Model	**Accuracy**	
	Total	**Ambiguous**
naive baseline	0.748	0.663
lstm8	0.936	0.915
blstm8	1.000	1.000
lstm8-nn8	0.936	0.915
blstm8-nn8	1.000	1.000
lstm8-lstm8-a8	1.000	1.000
blstm8-lstm8-a8	1.000	1.000

Table 5.3: Results of predicting the PoS tag with the synthetic dataset.

5.3. Wall Street Journal Dataset

In order to use the WSJ dataset, first we have to preprocess the corpus and make sure that the data introduced to the neural network is correct (section 5.3.1); after that, we conduct the experiments and evaluate the resulting neural networks (section 5.3.2).

5.3.1. Preprocessing

The WSJ dataset is composed of 25 sections, that we split in three sets. The first one is the training set and encompasses from section 0 to 18. The second one is the development set and encompasses from section 19 to section 21, and is used as a reference during training in order to apply early stopping (see section 2.4). The last one is the test set which encompasses from section 22 to section 24, and is used to evaluate the models. During the preprocessing of the original text files, we found several ambiguous words that were not disambiguated. As we follow a supervised training approach, sentences with non disambiguate words have been ignored.

As the development and test sets may contain unknown words not present in the training set, we created an ambiguity class for them. The PoS tags that belong to this ambiguity class are those corresponding to open lexical categories (see section 1.2).

After preprocessing the WSJ corpus, we analysed the distribution of unambiguous, ambiguous and unknown words in the three sets, and found out that about 2/3 of the words were ambiguous (including unknown words), which was wrong, because in English about 1/3 of the words in running texts are ambiguous (see section 1.2). As a consequence of that, we analysed the frequency of PoS tags for each word; for instance for the determiner "the" we obtained the next occurrences with the training set: { NNP:41, **DT:48875**, JJ:7, NN:1, CD:1, VB:1, VBP:1}; where several were incorrect, because "the" is not ambiguous and must always be assigned the PoS tag DT. In order to avoid the problem of words wrongly tagged, we only contemplate, for each word, the PoS tags with a frequency higher than 1% . The size of the vocabulary in training set is 39,471 words of which 381 words are assigned a PoS tags with a frequency lower than 1%. After applying this filtering, 237 words continued to be ambiguous and 144 ended not being so. The number of the ambiguity classes was reduced to 292 (before

applying the filtering there were 354). Table 5.4 shows the number of sentences in each set: sentences containing at least one word tagged incorrectly were omitted if they were ambiguous, otherwise they were substituted by the correspondent correct PoS tag. Table 5.5 and figure 5.9 shows the distribution of unambiguous, ambiguous and unknown word in each set, before and after the filter.

Set	**Sentences**		**Max length**	
	BF	**AF**	**BF**	**AF**
Training	40,084	39,542	250	
Development	6,109	6,011	111	
Test	7,025	6,915	118	

Table 5.4: Information about the sentences in the WSJ dataset, before (BF) and after (AF) the filter.

Set	**Words**		**Ambiguous words**		**Unknown words**	
	BF	**AF**	**BF**	**AF**	**BF**	**AF**
Training	968,458	951,005	606,272	328,927	0	
Development	147,883	144,930	94,745	52,770	4,170	4,102
Test	170,886	167,483	110,900	61,785	4,066	3,976

Table 5.5: Information about words in the WSJ dataset, before (BF) and after (AF) the filter.

5.3.2. Results

Table 5.7 shows NN setup of the trained model used in these experiments with WSJ corpus. All of them use bidirectional LSTM, with the exception of the encoder of one Seq2Seq experiment and both decoders of the Seq2Seq which use unidirectional LSTM. Dropout is used with a keep probability of 0.5; it is applied in all LSTMs and the *feedforward* NNs. The optimizer chosen is Adam with a learning rate of 0.003 and the size of the batch is 256.

As can been seen in table 5.6 the results of the baselines on the development and test sets are very close. The three baselines obtain the same accuracy with respect to unknown, because they use the same method to tag them.

Table 5.8 shows the results of predicting the next ambiguity class; with a large number of LSTM units, better results are obtained; however, in table 5.9, where the results of predicting PoS tag are reported, it can be seen that a high number of neurons

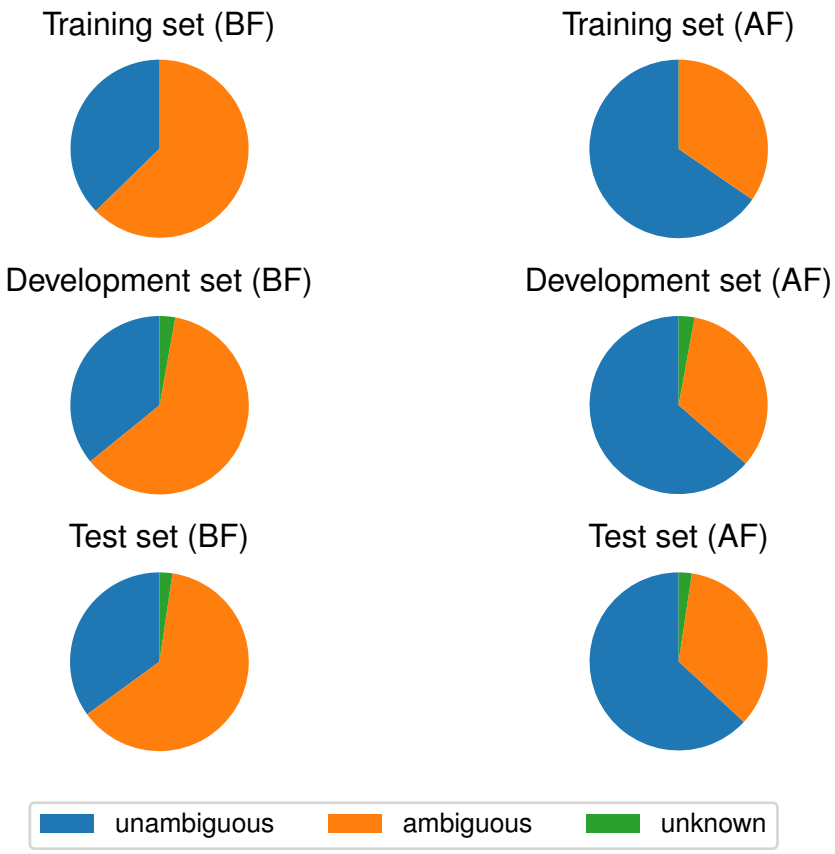

Figure 5.9: Distributions of unambiguous, ambiguous and unknown words in the WSJ dataset, before (BF) and after (AF) the filter.

Baseline	**Accuracy**					
	Total		**Ambiguous**		**Unknown**	
	Dev	**Test**	**Dev**	**Test**	**Dev**	**Test**
Tag level	0.818	0.816	0.513	0.512	0.157	0.120
Ambiguity level	0.871	0.873	0.659	0.665	0.157	0.120
Word level	0.901	0.902	0.741	0.743	0.157	0.120

Table 5.6: Baselines results with the WSJ dataset.

Architectures								
RNN	**Type**	**Layers**	**Units**	**Model name**				
	Bi-LSTM	1	64	blstm64-d0.5				
			128	blstm128-d0.5				
Two phases	**Phase 1: RNN**			**Phase 2: feedforward NN**		**Model name**		
	Type	**Layers**	**Units**	**Hidden layers**	**Units**			
	Bi-LSTM	1	256	1	64	blstm256-nn64-d0.5		
			512			blstm512-nn64-d0.5		
Seq2Seq	**Encoder**			**Decoder**			**Attention**	**Model name**
	Type	**Layers**	**Units**	**Type**	**Layers**	**Units**	**Units**	
	LSTM	1	64	LSTM	1	64	64	lstm64-lstm64-a64-d0.5
	Bi-LSTM							blstm64-lstm64-a64-d0.5

Table 5.7: NN setup used with the WSJ dataset.

in the RNN of the first phase, does not result in better accuracy in the second phase: the performance of both models are very close and the same happens with RNN architecture. However, the two models trained with Seq2Seq do not obtain similar results, because one uses a bidirectional encoder and the other uses an unidirectional encoder, unlike synthetic dataset (see section 5.2.5) in which both trained models obtained almost identical results. Therefore, with WSJ dataset a bidirectional Seq2Seq encoder surpasses an unidirectional Seq2Seq performance, as commented in section 2.3.4. The problem of these models is the accuracy obtained for the unknown ambiguity class, since the training corpus does not contain unknown words. However, the architecture in two phase obtains better results than the other two architectures (RNN and Seq2Seq architectures), because learning to predict the next ambiguity class helps to predict the PoS of unknown words. Furthermore, the results obtained on both sets (development and test) are very similar, guaranteeing does the absence of overfitting.

All the models shown in table 5.7 outperform results obtained by naive baselines, except Seq2Seq, possibly because we implemented a *greedy search* rather than a *beam search*, as it is usually done.

Model	**Cost**		**Accuracy**	
	Dev	**Test**	**Dev**	**Test**
blstm256-nn64-d0.5	2.416	2.400	0.684	0.687
blstm512-nn64-d0.5	1.902	1.882	0.826	0.832

Table 5.8: Results of predicting next ambiguity class on the WSJ dataset.

Model	**Cost**		**Total**		**Ambiguous**		**Unknown**	
	Dev	**Test**	**Dev**	**Test**	**Dev**	**Test**	**Dev**	**Test**
blstm64-d0.5	0.290	0.268	0.921	0.923	0.795	0.801	0.106	0.121
blstm128-d0.5	0.274	0.257	0.919	0.921	0.789	0.794	0.124	0.147
blstm256-nn64-d0.5	0.215	0.208	0.934	0.934	0.832	0.829	0.542	0.544
blstm512-nn64-d0.5	0.209	0.203	0.935	0.935	0.834	0.832	0.567	0.562
seq64-seq64-a64-d0.5	1.107	0.968	0.803	0.820	0.656	0.673	0.079	0.067
bseq64-seq64-a64-d0.5	0.606	0.547	0.887	0.893	0.753	0.762	0.053	0.044

Table 5.9: Results of predicting PoS tag on the WSJ dataset.

Figure 5.10 shows the cost and accuracy obtained for the first task by the architecture in two phases during training. As can be seen, the number of epochs needed when applying early stopping to learn the task with a high confidence is very low: two epoch in the model with 256 LSTM units and only one in the model with 512 LSTM units.

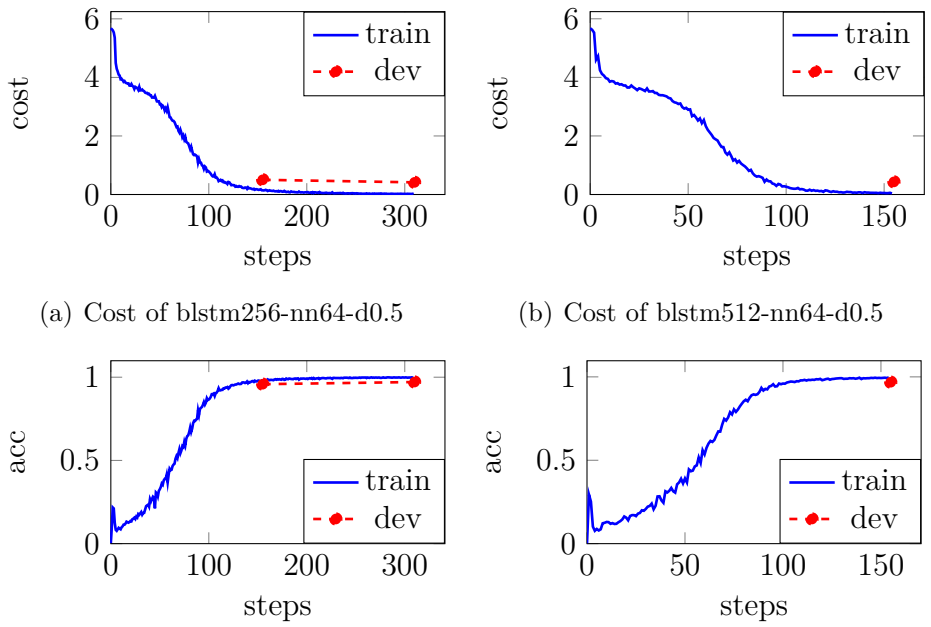

(a) Cost of blstm256-nn64-d0.5

(b) Cost of blstm512-nn64-d0.5

(c) Accuracy of blstm256-nn64-d0.5

(d) Accuracy of blstm512-nn64-d0.5

Figure 5.10: Results of the architecture in two phases on the first phase using the WSJ dataset.

As happens with results on the synthetic dataset (see section 5.2.5) the final accuracy obtained on the first task has been reduced in order to minimize the cost of learning the second task (see table 5.8).

Figure 5.11 shows the results obtained on the second task by the architecture in two phases during training. As can be seen in figures 5.12 and 5.13 the number of epochs needed by RNN architecture and Seq2Seq architecture are very large compared to architecture in two phases, which practically needs only one epoch or two epoch depending on the model trained, obtaining less cost and high accuracy than the models of the other two architectures.

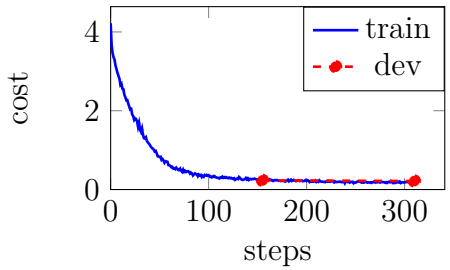

(a) Cost of blstm256-nn64-d0.5

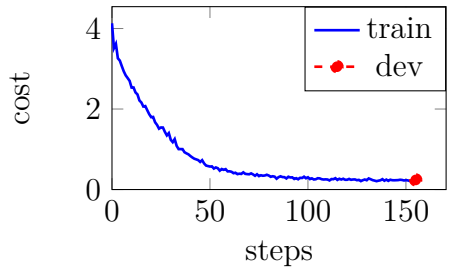

(b) Cost of blstm512-nn64-d0.5

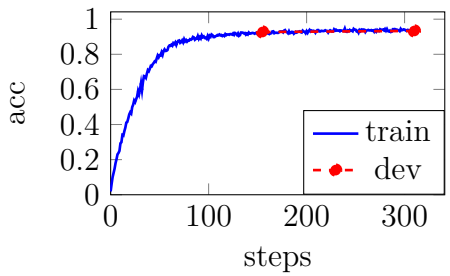

(c) Accuracy of blstm256-nn64-d0.5

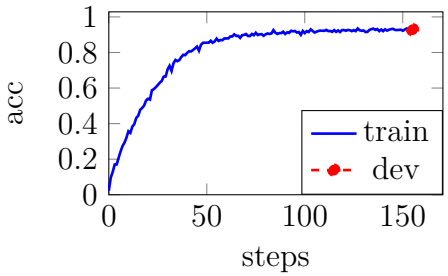

(d) Accuracy of blstm512-nn64-d0.5

Figure 5.11: Results of the architecture in two phases predicting PoS tag using the WSJ dataset.

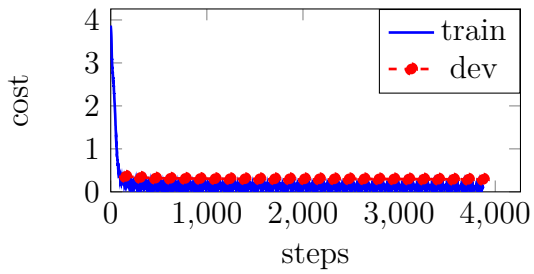

(a) Cost of blstm64-d0.5

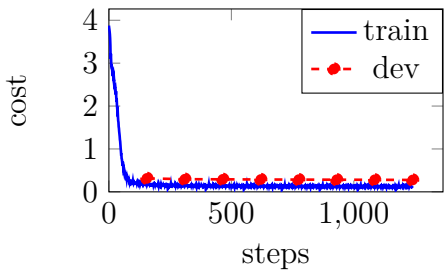

(b) Cost of blstm128-d0.5

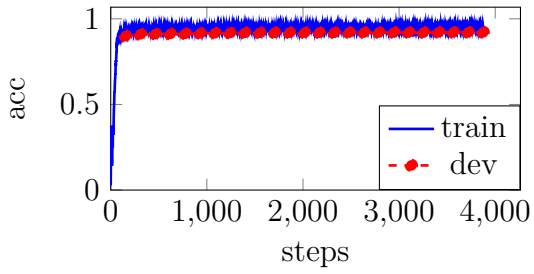

(c) Accuracy of blstm64-d0.5

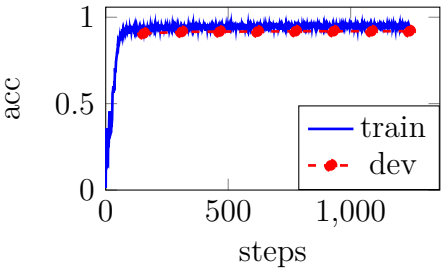

(d) Accuracy of blstm128-d0.5

Figure 5.12: Results of the RNN architecture on the WSJ dataset.

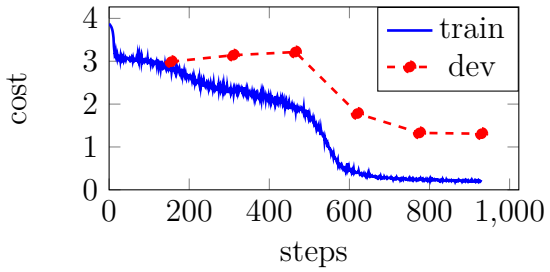

(a) Cost of seq64-seq64-a64-d0.5

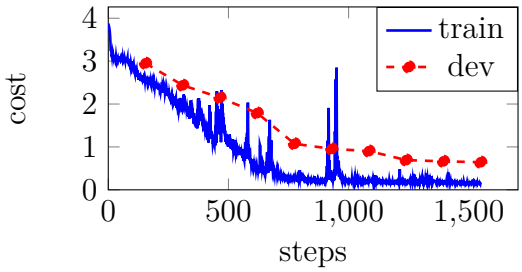

(b) Cost of bseq64-seq64-a64-d0.5

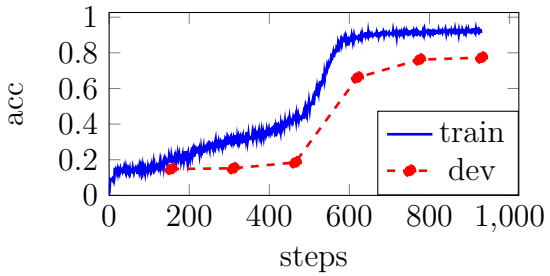

(c) Accuracy of seq64-seq64-a64-d0.5

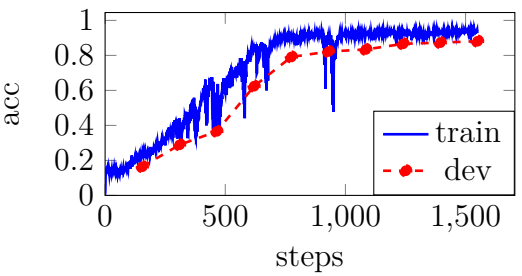

(d) Accuracy of bseq64-seq64-a64-d0.5

Figure 5.13: Results of the Seq2Seq architecture on the WSJ dataset.

Chapter 6

Conclusions

6.1. Conclusion

In this work, we have explored different approaches to PoS tagging. Additionally, we have explored different representations of the word classes in order to feed them as input into the model. Also, we have performed an exhaustive theoretical study of NN, specifically of sequence models like RNN and Seq2Seq. With all that background, we have proposed three architectures in order to tackle the problem of PoS tagging. Firstly, we experimented with a synthetic dataset generated by us that tries to imitate a real one, in order to ensure our implementations worked correctly. Finally, we experimented with different configurations of the proposed architectures on the WSJ corpus and we achieved a system able to disambiguate with a 93.5% total accuracy and with 83.2% accuracy on ambiguous words. Our results do not equal the state of the art in *part-of-speech* tagging on this dataset that is around 97% total accuracy [16]. We use one of the first version of WSJ. As can be seen in section 5.3.1, the corpus contains words tagged incorrectly. Probably, the preprocessing of the corpus used by us has been affect to do not achieve a performance close to 97% total accuracy, also those systems use the last version of WSJ corpus in which contains less mistakes and use more elaborated representations of the words than ours.

6.2. Highlights

The highlights of the work are the following:

- In-depth study of the neural models.
- Configuration of computing instances at GCP for DL research.
- Neural *part-of-speech* system implemented with TensorFlow. It allows to train whatever model that follows the proposed architectures described in this project, given a JSON file with the desired configuration. Once the models have been trained, they may be evaluated with a test set or used to disambiguate a raw text.

6.3. Future work

Due to the time constraints imposed on this project, many possible improvements were left out for future works. Here we summarize them:

- Complete the implementation of the Seq2Seq, since it actually uses a *greedy search* at inference mode instead of a *beam search* approach.
- Explore other approaches to represent unknown words, since the results obtained in this aspect are not good enough.
- Experiment with other hyperparameters and configurations.
- Calculate tests of statistical significance in order to know which is the best trained model.
- Include an unsupervised approach. In the training of this approach given an ambiguity class as input, its desired output will be its corresponding *multi-hot* representation in which all possible PoS tags have the same probability.

Bibliography

[1] Learning Phrase Representations using RNN Encoder–Decoder for Statistical Machine Translation.

[2] Dzmitry Bahdanau, Kyunghyun Cho, and Yoshua Bengio. Neural machine translation by jointly learning to align and translate. In *ICLR*, 2015.

[3] Yoshua Bengio, Patrice Simard, and Paolo Frasconi. Learning long-term dependencies with gradient descent is difficult. *IEEE Transactions on Neural Networks*, 5(2):157–166, 1994.

[4] Eric Brill. A Simple Rule-Based Part of Speech Tagger. Technical report.

[5] Eric Brilp. Unsupervised Learning of Disambiguation Rules for Part of Speech Tagging. Technical report.

[6] Doug Cutting, Julian Kupiec, Jan Pedersen, and Penelope Sibun. A Practical Part-of-Speech Tagger. Technical report.

[7] Geoffrey E Hinton David E Rumelhart and Ronald J Williams. Learning representations by back-propagating errors. *Cognitive modeling*, 5(3):1, 1988.

[8] Minh-Thang Luong Quoc Le Denny Britz, Anna Goldie. Massive exploration of neural machine translation architectures. *arXiv preprint arXiv:1703.03906*, 2017.

[9] Alex Krizhevsky Ilya Sutskever Ruslan R. Salakhutdinov Geoffrey E. Hinton, Nitish Srivastava. Improving neural networks by preventing co-adaptation of feature detectors. *arXiv preprint arXiv:1207.0580*, 2012.

[10] Alex Graves, Abdel-rahman Mohamed, and Geoffrey Hinton. Speech Recognition with Deep Recurrent Neural Networks. *ICASSP, IEEE International Conference on Acoustics, Speech and Signal Processing - Proceedings*, (3):6645–6649, 2013.

[11] Andreas Griewank. Automatic differentiation of algorithms: theory, implementation, and application. *In proceedings of the first SIAM Workshop on Automatic Differentiation*, pages 1045–1048, 1991.

[12] Sepp Hochreiter and Jürgen Schmidhuber. Long short-term memory. *Neural Computation*, 9(8):1735–1780, 1997.

[13] Daniel Jurafsky and James H. Martin. *Speech and Language Processing (3rd Edition)*.

[14] D. P. Kingma and J. Ba. Adam: A method for stochastic optimization. *arXiv preprint arXiv:1609.04747*, 2014.

[15] Maxwell Stinchcombe Kurt Hornik and Halbert White. Multilayer feedforward networks are universal approximators. *Neural networks*, 2(5):359–366, 1989.

[16] Christopher D Manning. Part-of-Speech Tagging from 97 % to 100 %: Is It Time for Some Linguistics ?

[17] Santorini B. Marcus, M. P. and M. A Marcinkiewicz. Building a large annotated corpus of english: The penn treebank. *Computational Linguistics*, 19(2):313–330, 1993.

[18] Paul Barham Eugene Brevdo Zhifeng Chen Craig Citro Greg S Corrado Andy Davis Jeffrey Dean Matthieu Devin Martın Abadi, Ashish Agarwal. Tensorflow: Large-scale machine learning on heterogeneous distributed systems. *arXiv preprint arXiv:1603.04467*, 2016.

[19] Andrei Mikheev. Unsupervised learning of word-category guessing rules. In *Proceedings of the 34th Annual Meeting of the Association for Computational Linguistics, New York, NY*, page 327–333, 1996.

[20] Samy Bengio Dumitru Erhan Oriol Vinyals, Alexander Toshev. Show and Tell: A Neural Image Caption Generator. nov 2014.

[21] Razvan Pascanu, Tomáš Mikolov, and Yoshua Bengio. On the difficulty of training recurrent neural networks. In *ICML*, 2013.

[22] Juan Antonio Pérez-Ortiz and M. L. Forcada. Part-of-speech tagging with recurrent neural networks. In *IJCNN*, 2001.

[23] Adwait Ratnaparkhi. A Maximum Entropy Model for Part-Of-Speech Tagging. Technical report.

[24] S Ruder. An overview of gradient descent optimization algorithms. *arXiv preprint arXiv:1609.04747*, 2016.

[25] Hehnut Schmid. Part-of-speech tagging with neural networks. Technical report.

[26] Ilya Sutskever, Oriol Vinyals, and Quoc V. Le. Sequence to sequence learning with neural networks. In *NIPS*, 2014.

[27] Felipe Sánchez-Martinez. Part-of-speech tagging. *Routledge Encyclopedia of Translation Technology*, 36(1):594–604, 2014.

[28] Nosratola D. Vaziri, Jun Yuan, Ardeshir Rahimi, Zhenmin Ni, Hyder Said, and Veedamali S. Subramanian. Disintegration of colonic epithelial tight junction in uremia: A likely cause of CKD-associated inflammation. *Nephrology Dialysis Transplantation*, 27(7):2686–2693, 2012.

[29] R.E. Wengert. A simple automatic derivative evaluation program. *Communications of the ACM*, 7(8):463–464, 1964.

[30] Paul J. Werbos. Back propagation through time: What it does and how to do it. In *Proceedings of the IEEE*, volume 78, pages 1550–1560, 1990.

[31] Sam Wiseman and Alexander M. Rush. Sequence-to-sequence learning as beam-search optimization. In *EMNLP*, 2016.

[32] Yuan; Lorenzo Rosasco; Andrea Caponnetto Yao. On early stopping in gradient descent learning. *Constructive Approximation*, 26(2):289–315, 2007.